

Synthesis of (Adamantylimido)vanadium(V) Dimethyl Complex Containing (2-Anilidomethyl)pyridine Ligand and Selected Reactions: Exploring the Oxidation State of the Catalytically Active Species in Ethylene Dimerization

Kotohiro Nomura,^{*,†} Takato Mitsudome,^{*,‡} Atsushi Igarashi,[†] Go Nagai,[†] Ken Tsutsumi,[†] Toshiaki Ina,[§] Takuya Omiya,[†] Hikaru Takaya,^{*,||} and Seiji Yamazoe^{*,⊥}

[†]Department of Chemistry, Faculty of Science and Engineering, Tokyo Metropolitan University, 1-1 Minami Osawa, Hachioji, Tokyo 192-0397, Japan

[‡]Department of Materials Engineering Science, Osaka University, 1-3, Machikaneyama, Toyonaka, Osaka 560-8531, Japan

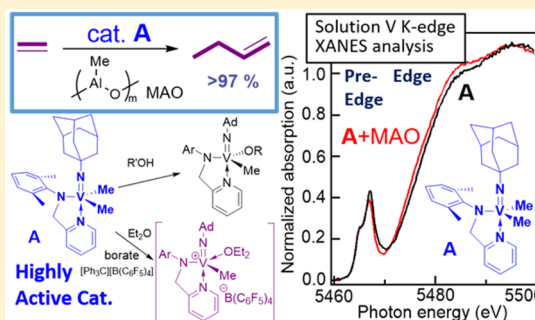
[§]Japan Synchrotron Radiation Research Institute (JASRI, SPring-8), Sayo, Hyogo 679-5198, Japan

^{||}International Research Center for Elements Science (IRCELS), Institute for Chemical Research (ICR), Kyoto University, Uji, Kyoto 611-0011, Japan

[⊥]Department of Chemistry, School of Science, The University of Tokyo, 7-3-1 Hongo, Bunkyo-ku, Tokyo 113-0033, Japan

Supporting Information

ABSTRACT: V(NAd)Me₂(L) [**2a**, L = 2-ArNCH₂(C₅H₄N), Ar = 2,6-Me₂C₆H₃], prepared from V(NAd)Cl₂(L) (**1**) by reaction with LiMe (2.0 equiv), exhibited remarkable catalytic activities for ethylene dimerization in the presence of MAO affording 1-butene with high selectivity [TOF = 1 120 000–1 530 000 h⁻¹ (311–425 s⁻¹), C₄' = 97.1–98.4%], and the catalyst performances (activity, selectivity) were similar to those by the dichloride analogue (**1**) under the same conditions. The dimethyl complex (**2a**) reacted with 1.0 equiv of R'OH to yield the mono alkoxide complexes, V(NAd)Me(OR')(L) [R' = OC(CF₃)₃ (**3a**), OC(CH₃)(CF₃)₂ (**3b**), OC(CH₃)₃ (**3c**)], and structures of these complexes (**3a–c**) and **2a** were determined by X-ray crystallography. Reactions of **2a** with [Ph₃C][B(C₆F₅)₄] in Et₂O and **3c** with B(C₆F₅)₃ in THF afforded the corresponding cationic complexes confirmed by NMR spectra. Both NMR and V K-edge XANES analysis of the toluene or toluene-*d*₈ solution of **1** and **2a** did not show any significant changes in the oxidation state upon addition of MAO, Me₂AlCl, or Et₂AlCl (10 equiv). Resonances ascribed to formation of the other vanadium(V) species were observed in the ⁵¹V NMR spectra, and no significant differences in the XANES spectra (V–K pre-edge peaks and edge) were observed from **1** or **2a** upon addition of Al cocatalyst. Taking into account these results and others, it is thus suggested that cationic vanadium(V) alkyl/hydride species play a role in this catalysis.



INTRODUCTION

Ethylene oligomerization, exemplified by nickel complex catalyst containing a chelate P–O ligand (shell higher olefin process, SHOP),^{1,2} for production of linear α -olefins (intermediates such as detergents, polymers, lubricants, surfactants, etc.) is one of the important key reactions in chemical industry.¹ The subject concerning design of the efficient (highly active and selective) catalysts thus attract considerable attention;^{2–12} examples for ethylene oligomerization especially using nickel,^{2,4} iron complex catalysts,⁵ or ethylene trimerization especially using chromium^{6–8} or titanium complex catalysts⁹ have been well-known. Two reaction mechanisms via metal–hydride (or metal–alkyl) or metallacycle intermediate have been postulated in the ethylene oligomerization; the latter mechanism can be especially considered for the selective trimerization (and tetramerization)

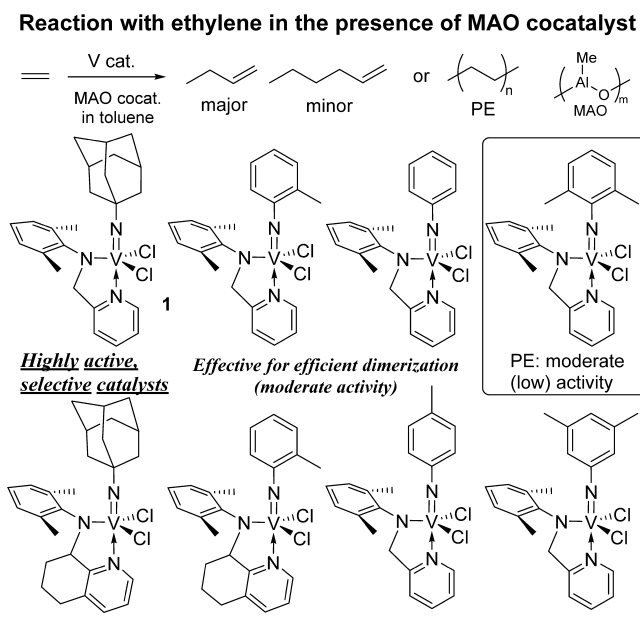
affording 1-hexane (and 1-octene) with high selectivity. Since metal–alkyl or metal–hydride plays an important role in the former mechanism, synthesis and reaction chemistry of metal–alkyl species have thus been an important subject for better understanding in the mechanism as well as of organometallic chemistry.

Recently, we demonstrated that (imido)vanadium(V) complexes containing (2-anilidomethyl)pyridine or 8-anilido-5,6,7-trihydroquinoline ligands, V(NR)Cl₂[2-ArNCH₂(C₅H₄N)] or V(NR)Cl₂[8-Ar-N(C₉H₁₀N)] [R = 1-adamantyl (Ad), 2-MeC₆H₄, C₆H₅, etc.; Ar = 2,6-Me₂C₆H₃], exhibited high catalytic activities and selectivities for ethylene dimerization in the presence of methylaluminoxane (MAO)

Received: September 13, 2016

cocatalyst (Scheme 1).¹² Through this study, it turned out that a steric bulk in the imido ligand directly affects the ethylene

Scheme 1. Effect of Ligand Substituents in Ethylene Dimerization/Polymerization (MAO Cocatalyst): Selected Examples for Effective Catalysts^{12a,c,d}



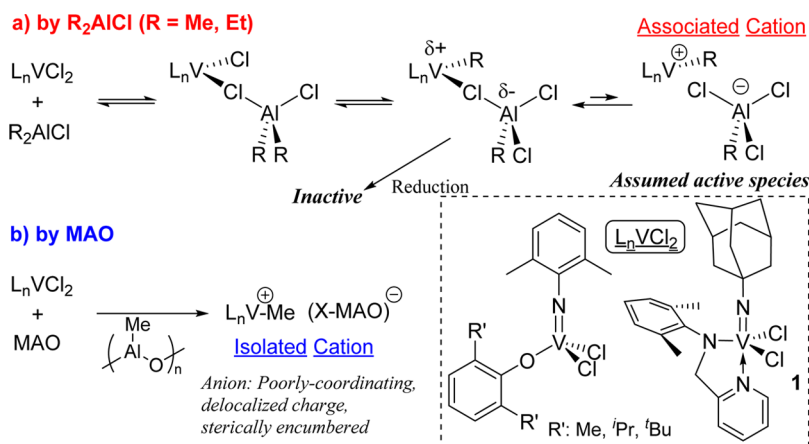
reactivity (between dimerization and polymerization). 2,6-Dimethylphenylimido analogue, $V(N-2,6-Me_2C_6H_3)Cl_2[2-ArNCH_2(C_5H_4N)]$, showed the moderate activity for ethylene polymerization, whereas not only the adamantylimido analogues, $V(NAd)Cl_2[2-ArNCH_2(C_5H_4N)]$ (**1**), but also the cyclohexylimido, phenylimido, and *o*-tolylimido analogues afforded 1-butene with high selectivity (Scheme 1).^{12a,c} It also turned out that an electronic factor in the imido ligand would affect the catalytic activity; the adamantylimido analogues (**1**, etc.) exhibited the higher catalytic activities.^{12a} More recently, we reported that (imido)vanadium complexes containing 8-(2,6-dimethylanilide)-5,6,7-trihydroquinoline ligands exhibited higher catalytic activities with high selectivity for ethylene dimerization.^{12d}

Moreover, it also turned out that the reaction pathway with ethylene (dimerization vs polymerization) is highly affected by

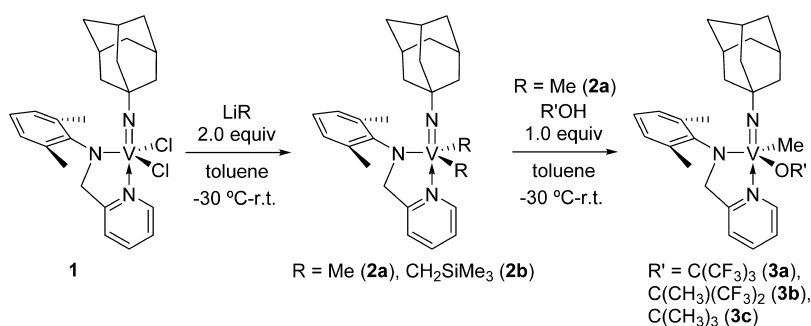
Al cocatalyst employed. Reaction with ethylene by **1** in the presence of MAO, MMAO afforded 1-butene as the major product, whereas the reaction in the presence of Me_2AlCl , Et_2AlCl afforded polyethylene with ultrahigh molecular weights.^{12b} On the basis of our previous assumption observed in the ethylene/norbornene copolymerization using (imido)-vanadium(V) dichloride complexes containing aryloxo ligands, $V(N-2,6-Me_2C_6H_3)Cl_2(OAr)$,^{13,14} in which both the activity and norbornene incorporations were highly affected by Al cocatalyst (and solvent) employed,^{13b,c,14e} we speculated that a reason for the observed difference would be due to a formation of different catalytically active species and catalyst/cocatalyst nuclearity¹⁵ in the two catalyst systems (assumed in Scheme 2).^{12b}

As mentioned above, two reaction mechanisms via metal-hydride (or metal-alkyl) or metallacycle intermediate in the ethylene oligomerization can be considered, and the above results (effect of Al cocatalyst toward the ethylene reactivity) and the results in ethylene pressure dependence (first order toward the activity) would strongly suggest a possibility of metal-hydride (alkyl) intermediates in this catalysis.^{12b} Moreover, no (or trace amount of) resonances ascribed to paramagnetic [vanadium(IV)] species were observed in the ESR spectra of toluene solution containing **1** in the presence of Al alkyls (MMAO, Et_2AlCl , 100 equiv to V), whereas the resonances ascribed to a paramagnetic species [vanadium(IV) species]^{16–18} were observed when $V(NAd)Cl_3$ was treated with Et_2AlCl (100 equiv). Similarly, another broad resonance was observed in the ^{51}V NMR spectra of C_6D_6 solution containing **1** in the presence of 10.0 equiv of MMAO or Et_2AlCl (25 °C), whereas no resonances were observed when $V(NAd)Cl_3$ was treated with 10.0 equiv of Et_2AlCl (under the same concentration in C_6D_6 at 25 °C), suggesting a formation of paramagnetic species as observed in the ESR resonance. These ESR and NMR results suggest that the anionic donor ligand plays an essential role for stabilization of the oxidation state, vanadium(V), even in the catalyst solution. Although these results would also suggest a possibility that the cationic vanadium(V)-alkyl species play an important role in this catalysis, however, we need to provide more clear evidence concerning the catalytically active species (especially oxidation state). This is because that in the classical Ziegler-type catalyst systems [$V(acac)_3$, $VOCl_3$, etc., and Et_2AlCl , $EtAlCl_2$, $nBuLi$, etc.], which display unique high reactivity toward olefins in

Scheme 2. Assumed Catalytically Active Species Formed by Reaction with Al Alkyls



Scheme 3. Synthesis of Dialkyl Complexes $V(\text{NAd})\text{R}_2[2\text{-ArNCH}_2(\text{C}_5\text{H}_4\text{N})]$ [$\text{R} = \text{Me}$ (**2a**), CH_2SiMe_3 (**2b**)] and Reactions of **2a** with Alcohols



olefin coordination/insertion polymerization,^{19–22} vanadium(III) and/or vanadium(IV) species are proposed to be as the catalytically active species (although the catalyst systems require addition of reoxidant such as $\text{Cl}_3\text{CCO}_2\text{Et}$ to stabilize the oxidation state of the active species).^{14,23}

As described above, since metal-alkyl, especially cationic alkyl species, plays an important role in catalysis in ethylene dimerization/polymerization, we thus explored a possibility for isolation of the corresponding dimethyl and the cationic methyl complexes and some reactions. We also explored possibilities to obtain clear supports by *in situ* analysis (of catalyst solution in toluene) for better explanation of our proposed mechanism. We thus herein present synthesis of the dimethyl complex, $V(\text{NAd})\text{Me}_2[2\text{-ArNCH}_2(\text{C}_5\text{H}_4\text{N})]$ (**2a**), and some reactions including structural analyses by X-ray crystallography. Moreover, we explored analysis of the catalyst solution in the presence of Al cocatalysts by ^{51}V NMR spectra and solution XAS (X-ray absorption spectroscopy) analysis. Through these results, we wish to demonstrate that the chelate anionic donor ligand plays an essential role for stabilization of the oxidation state for exhibiting both high catalytic activity and selectivity in ethylene dimerization.

RESULTS AND DISCUSSION

Synthesis and Structural Analysis of $V(\text{NAd})\text{R}_2[2\text{-ArNCH}_2(\text{C}_5\text{H}_4\text{N})]$ [$\text{R} = \text{Me}$ (2a**), CH_2SiMe_3 (**2b**)] and Some Reactions.** Reactions of $V(\text{NAd})\text{Cl}_2[2\text{-ArNCH}_2(\text{C}_5\text{H}_4\text{N})]$ (**1**, $\text{Ar} = 2,6\text{-Me}_2\text{C}_6\text{H}_3$) with 2.0 equiv of LiMe or $\text{LiCH}_2\text{SiMe}_3$ in toluene gave the dialkyl analogues, $V(\text{NAd})\text{R}_2[2\text{-ArNCH}_2(\text{C}_5\text{H}_4\text{N})]$ [$\text{R} = \text{Me}$ (**2a**), CH_2SiMe_3 (**2b**)] (Scheme 3), and these complexes were identified by ^1H , ^{13}C , and ^{51}V NMR spectra and elemental analysis, and the structure of **2a** could be determined by X-ray crystallography (shown below, Figure 1).²⁴ Resonance ascribed to the methyl protons (0.92 ppm) was observed in the ^1H NMR spectrum of **2a**, whereas resonances ascribed to the SiMe_3 group (0.12 ppm) in addition to the methylene (2.57 ppm) were observed in the ^1H NMR spectrum of **2b**.

Reactions of **2a** with 1.0 equiv of $(\text{CF}_3)_3\text{COH}$, $(\text{CH}_3)_3\text{COH}$, $(\text{CF}_3)_2(\text{CH}_3)\text{COH}$ in toluene afforded the corresponding mono alkoxo complexes, $V(\text{NAd})\text{Me}(\text{OR}')[2\text{-ArNCH}_2(\text{C}_5\text{H}_4\text{N})]$ [$\text{R}' = \text{OC}(\text{CF}_3)_3$ (**3a**), $\text{OC}(\text{CH}_3)(\text{CF}_3)_2$ (**3b**), $\text{OC}(\text{CH}_3)_3$ (**3c**)], in high yields (Scheme 3). These complexes were identified by ^1H , ^{13}C , ^{19}F , and ^{51}V NMR spectra, and their structures (**3a–c**) were determined by X-ray crystallography (shown in Figure 1).²⁴

Figure 1 shows ORTEP drawings for complexes **2a** and **3a–c**, and the selected bond distances and angles are summarized

in Table 1.²⁴ Dimethyl complex **2a** folds trigonal bipyramidal geometry around vanadium with the pyridyl N donor of the bidentate (2-anilidomethyl)-pyridine ligand and the imido N atom lying on the axis, and an equatorial plane consisted of the two methyl ligands and the anilido N atom. The axial $\text{N}(1)\text{–V–N}(2)$ bond angle [$177.73(8)^\circ$] is larger than that in the chloride analogue (**1**) [$174.90(4)^\circ$],^{12a} and the sum of the equatorial $\text{C}(25)\text{–V–C}(26)$, $\text{C}(25)\text{–V–N}(3)$, and $\text{C}(26)\text{–V–N}(3)$ bond angles is 354.94° . Moreover, the nitrogen atom in the pyridine locates at *trans*-position of the imido ligand [$\text{N}(1)\text{–V–N}(2)$: $177.73(8)^\circ$], and the $\text{V–N}(1)\text{–C}(1)$ bond angle [$176.36(15)^\circ$] is also larger than that in (**1**) [$170.94(10)^\circ$],^{12a} clearly suggesting that complex **2a** folds in a linear structure from $\text{C}(1)$ through $\text{N}(2)$. The V–C bond distances in **2a** [$2.092(4)$, $2.091(5)$ Å] are somewhat longer than that in reported $V(\text{N}-2,6\text{-Me}_2\text{C}_6\text{H}_3)\text{Me}(\text{NC}^t\text{Bu}_2)_2$ [$2.064(2)$ Å]²⁵ and V–C bond distances in $V(\text{NAd})(\text{CH}_2\text{SiMe}_3)_3$ [$2.0267(18)$ Å],²⁶ $V(\text{CHSiMe}_3)(\text{NAd})(\text{CH}_2\text{SiMe}_3)(\text{NHC})$ [$2.069(3)$ Å, $\text{NHC} = 1,3\text{-bis}(2,6\text{-diisopropylphenyl})\text{-imidazol-2-ylidene}$],²⁶ but within the range of the V–C bond lengths in (arylimido)vanadium(V)-dibenzyl analogues [$2.026(7)\text{–}2.103(8)$ Å].²⁷ The $\text{C}(25)\text{–V–C}(26)$ bond angle [$116.81(13)^\circ$] is smaller than $\text{Cl}(1)\text{–V–Cl}(2)$ bond angle in **1** [$119.953(16)^\circ$].^{12a} The $\text{V–N}(3)$ bond distance in **2a** [$1.886(3)$ Å] is apparently longer than that in **1** [$1.8580(12)$ Å] as well as those in the other (imido)vanadium(V) dichloride analogues with different imido ligands, $V(\text{NR})\text{Cl}_2[2\text{-Ar'NCH}_2(\text{C}_5\text{H}_4\text{N})]$ [$\text{R} = \text{Ad}$, cyclohexyl, $2\text{-MeC}_6\text{H}_4$, $2,6\text{-Me}_2\text{C}_6\text{H}_3$; $\text{Ar}' = 2,6\text{-Me}_2\text{C}_6\text{H}_3$, $2,6\text{-}^i\text{Pr}_2\text{C}_6\text{H}_3$], reported previously [$1.850(2)\text{–}1.8607(18)$ Å].^{12a,c,28}

Structures of the methyl-mono alkoxide analogues, $V(\text{NAd})\text{Me}(\text{OR}')[2\text{-ArNCH}_2(\text{C}_5\text{H}_4\text{N})]$ [$\text{R}' = \text{OC}(\text{CF}_3)_3$ (**3a**), $\text{OC}(\text{CH}_3)(\text{CF}_3)_2$ (**3b**), $\text{OC}(\text{CH}_3)_3$ (**3c**)], are also shown in Figure 1.²⁴ Similarly, these complexes fold a distorted trigonal bipyramidal geometry around vanadium consisting of two nitrogen atoms in the pyridine and the imido ligands axis, and an equatorial plane consisted of one methyl and alkoxo ligands and the nitrogen in the anilido ligand [$\text{N}(1)\text{–V–N}(2) = 171.35(8)^\circ$ in **3a**, $171.01(10)^\circ$ in **3b**, $167.41(8)^\circ$ in **3c**; total bond angles of $\text{C}(25)\text{–V–O}(1)$, $\text{C}(25)\text{–V–N}(3)$, $\text{O}(1)\text{–V–N}(3)$: 350.48° in **3a**, 351.52° in **3b**, 351.83° in **3c**, respectively]; the nitrogen atom in the pyridine locates at the *trans*-position of the imido ligand. The vanadium–nitrogen bond distance in the anilido ligand and the $\text{V–O}(1)$ bond distance in **3a–c** are affected by the alkoxo substituents [$\text{V–N}(3)$, $\text{V–O}(1)$: $1.888(2)$, $1.8999(16)$ Å in **3a**; $1.907(3)$, $1.867(2)$ Å in **3b**; $1.9240(18)$, $1.8016(17)$ Å in **3c**, respectively]; the similar influence is also observed in the V–

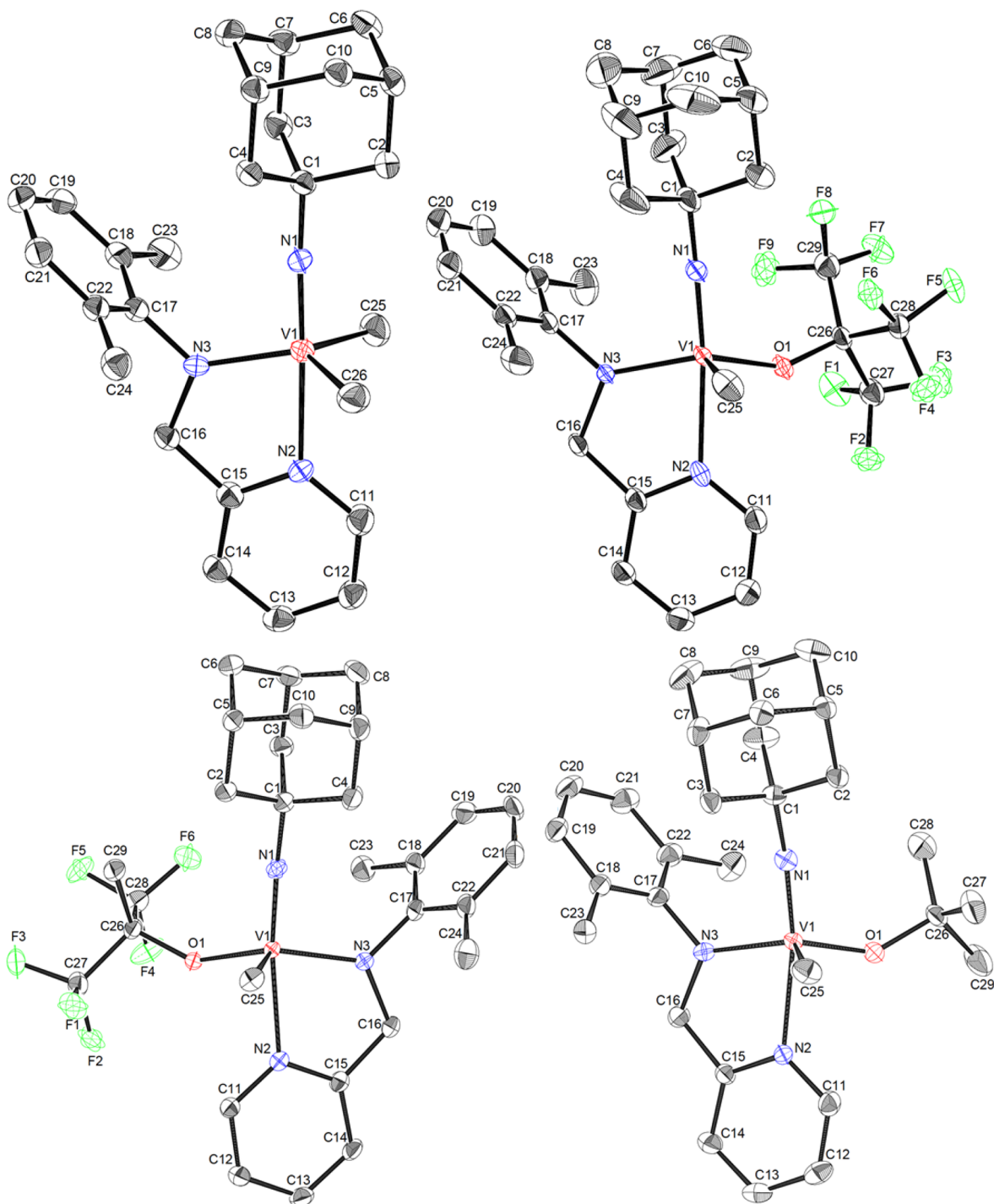


Figure 1. ORTEP drawing for $V(NAd)Me_2[2-(2,6-Me_2C_6H_3)NCH_2(C_5H_4N)]$ (**2a**, top left), $V(NAd)Me(OR')[2-(2,6-Me_2C_6H_3)NCH_2(C_5H_4N)]$ [$R = C(CF_3)_3$ (**3a**, top right), $C(CH_3)(CF_3)_2$ (**3b**, bottom left), and $C(CH_3)_3$ (**3c**, bottom right)]. Thermal ellipsoids are drawn at the 50% probability level, and H atoms are omitted for clarity.²⁴

$N(2)$ in pyridine bond distance [2.2243(17), 2.234(3), and 2.251(2) Å in **3a**, **3b**, and **3c**, respectively]. Moreover, $N(1)-V-N(2)$ and $V-N(1)-C(1)$ bond angles are also influenced by the alkoxy substituent [$N(1)-V-N(2)$, $V-N(1)-C(1)$: 171.35(8), 171.51(15)° in **3a**; 171.01(10), 170.4(3)° in **3b**; 167.41(8), 168.37(15)° in **3c**, respectively]. The bond angles in $C(25)-V-O(1)$, $N(2)-V-N(3)$, and $C(25)-V-N(3)$ are also influenced by the alkoxy ligand employed (Table 1). It seems likely that $V-O(1)$ bond distances in **3a-c** are influenced by the electronic (and probably steric) nature of

the alkoxy substituents, which would affect the $V-N(1)$, $V-N(3)$ distances and $N(1)-V-N(2)$, $V-N(1)-C(1)$ bond angles, among others.

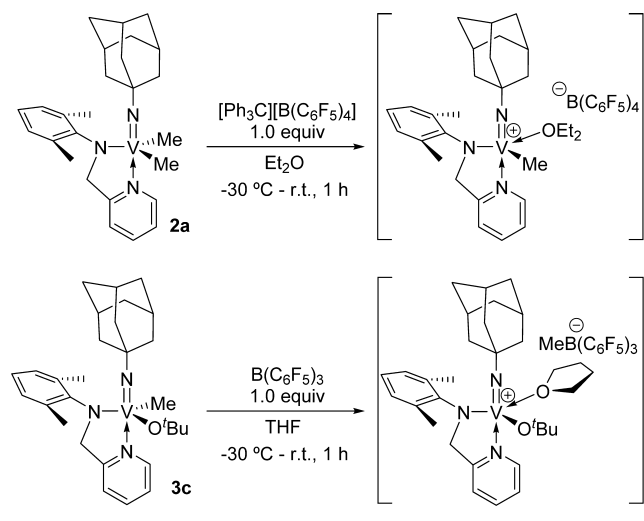
In order to obtain further information concerning the assumed catalytically active species, reaction of the dimethyl complex (**2a**) with 1.0 equiv of $[Ph_3C][B(C_6F_5)_4]$ was explored in Et_2O (Scheme 4).²⁹⁻³¹ After removal of volatiles, the resultant solid was washed with *n*-hexane and dried *in vacuo*. ^{51}V NMR spectrum of the resultant solid (in $CDCl_3$ at 25 °C, Figure 2b) showed a resonance at 83.6 ppm which is apparently

Table 1. Selected Bond Distances and Angles for V(NAd)Me₂[2-ArNCH₂(C₅H₄N)] (2a, Ar = 2,6-Me₂C₆H₃), V(NAd)Me(OR')[2-ArNCH₂(C₅H₄N)] [R' = C(CF₃)₃ (3a), C(CH₃)(CF₃)₂ (3b), and C(CH₃)₃ (3c)]^a

complex	1 ^b	2a	3a	3b	3c
Bond Distances (Å)					
V–N(1)	1.6517(12)	1.654(3)	1.6521(17)	1.662(3)	1.6642(19)
V–N(2)	2.2241(11)	2.221(3)	2.2243(17)	2.234(3)	2.251(2)
V–N(3)	1.8580(12)	1.886(3)	1.888(2)	1.907(3)	1.9240(18)
V–C(25)	2.2677(3), V–Cl(1)	2.092(4)	2.101(3)	2.099(4)	2.112(3)
V–C(26) or V–O(1)	2.2709(4), V–Cl(2)	2.091(5)	1.8999(16)	1.867(2)	1.8016(17)
Bond Angles (deg)					
V–N(1)–C(1)	170.94(10)	176.36(15)	171.51(15)	170.4(3)	168.37(15)
N(1)–V–N(2)	174.90(4), N(1)–V–N(3)	177.73(8)	171.35(8)	171.01(10)	167.41(8)
N(2)–V–N(3)	78.20(4), N(1)–V–N(2)	78.08(9)	77.24(7)	76.75(10)	75.46(8)
N(1)–V–N(3)	97.41(5), N(1)–V–N(3)	99.65(10)	98.13(9)	97.94(11)	98.30(9)
C(25)–V–O(1)	119.953(16), Cl(1)–V–Cl(2)	116.81(13), C(25)–V–C(26)	111.61(9)	108.78(12)	107.56(9)
C(25)–V–N(3)	116.92(4), Cl(1)–V–N(2)	118.11(12)	109.59(9)	113.69(11)	118.59(9)
O(1)–V–N(3)	118.18(3), Cl(2)–V–N(2)	120.02(12), C(26)–V–N(3)	129.28(7)	129.05(11)	125.68(8)

^aDetailed analysis data are shown in the Supporting Information.²⁴ ^bData for V(NAd)Cl₂[2-(2,6-Me₂C₆H₃)NCH₂(C₅H₄N)] (1) reprinted with permission in part from ref 12a. Copyright 2010 American Chemical Society.

Scheme 4. Reactions of V(NAd)Me₂[2-ArNCH₂(C₅H₄N)] (2a) with [Ph₃C][B(C₆F₅)₄] and V(NAd)Me(O^tBu)[2-ArNCH₂(C₅H₄N)] (3c) with B(C₆F₅)₃



different (shifted high magnetic field side) from that in the dimethyl complex (2a, 203.1 ppm, Figure 2a); 3 resonances ascribed to C₆F₅ group were also observed in the ¹⁹F NMR spectrum.³¹ Moreover, resonances ascribed to protons in Ph₃C(CH₃) (ca. 2.2 ppm),³² and a resonance ascribed to vanadium–methyl protons (1.53 ppm) was also observed in the ¹H NMR spectrum (in CDCl₃ at 25 °C, Figure 2d); most of all resonances were assigned to protons of an assumed cationic complex, [V(NAd)Me{2-ArNCH₂(C₅H₄N)}(Et₂O)]⁺, shown in Scheme 4.³¹ The similar reaction in C₆D₆ or toluene-*d*₈ afforded two separated solutions consisting of toluene-soluble portion (clear pale brown) and toluene-insoluble deep brown tan residue at the bottom. The observed small resonances (from the top clear brown solution) were ascribed to the starting complex (2a), and the amount (intensity) was significantly reduced from the initial charged amount. This is a similar observation in the reaction of Cp*TiMe₂(O-2,6-*i*-Pr₂C₆H₃) with [Ph₃C][B(C₆F₅)₄]^{33a} and the others,^{30a,33} suggesting a formation of cationic (alkyl) species.

Similarly, reaction of the O^tBu analogue (3c) with 1.0 equiv of B(C₆F₅)₃ was explored in THF (Scheme 4).^{31,33c} After removal of volatiles, the resultant solid was washed with *n*-hexane and dried *in vacuo*. ⁵¹V NMR spectrum of the resultant solid (in CDCl₃ at 25 °C) showed a resonance at –309.6 ppm which is clearly shifted from that in the mono methyl complex (3c, –246.5 ppm); 3 resonances ascribed to C₆F₅ group were also clearly observed in the ¹⁹F NMR spectrum.³¹ Moreover, resonance ascribed to the methyl group in (CH₃)B(C₆F₅)₃ (0.48 ppm) accompanied by disappearance of resonance ascribed to protons in vanadium–methyl (0.63 ppm) was observed; resonances ascribed to free and coordinated THF were also observed.³¹ These results would suggest a formation of cationic species, [V(NAd)(O^tBu){2-ArNCH₂(C₅H₄N)}(THF)]⁺, *in situ*, as shown in Scheme 4, although formation of the cationic complex was only suggested by NMR spectra (shown in the Supporting Information).³¹

Reactions of Ethylene by V(NAd)Me₂[2-ArNCH₂(C₅H₄N)] (2a) in the Presence of Cocatalyst.

Table 2 summarizes results for reaction with ethylene by V(NAd)Me₂[2-ArNCH₂(C₅H₄N)] (2a) in the presence of cocatalysts. The results by dichloride analogue V(NAd)Cl₂[2-ArNCH₂(C₅H₄N)] (1)^{12a,b} are also placed for comparison. As reported previously,^{12a,b} 1 showed remarkable both catalytic activity and selectivity for ethylene dimerization in the presence of MAO (runs 1–3),^{12a} whereas the reactions of 1 with ethylene in the presence of Me₂AlCl, Et₂AlCl afforded polyethylene with ultrahigh molecular weights (runs 4 and 5).^{12b}

It turned out that the dimethyl analogue (2a) exhibited remarkable catalytic activities for reaction with ethylene in the presence of MAO cocatalyst (runs 6–11). The products of those reactions conducted at rather low catalyst concentration conditions (2a 0.2 μmol, runs 8–11) were 1-butene with high selectivity (97.1–98.4%), whereas percentage of 1-hexene increased if the reactions were conducted under rather high catalyst concentration (2a 0.5 μmol; selectivity of 1-butene = 91.0, 87.9% for runs 6 and 7, respectively). As reported previously,^{12a,b} 1-hexene was formed after accumulation of 1-butene in the reaction mixture (ca. 7.49 g of 1-butene and 0.7 g of 1-hexene formed in 30 mL of toluene, run 6). Moreover, the activity was affected by the Al/V molar ratio employed. These

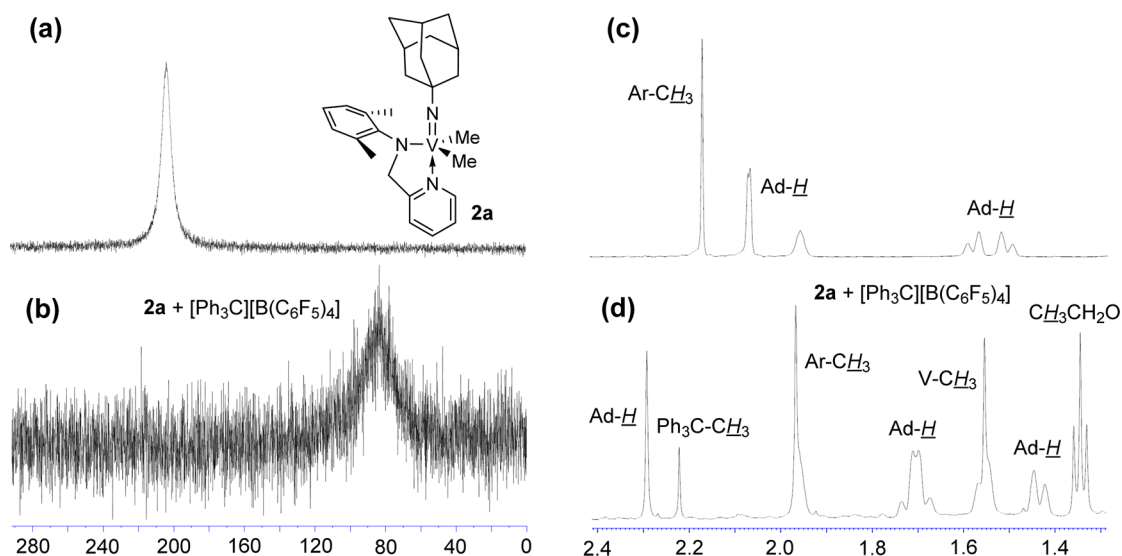


Figure 2. ^{51}V NMR spectra (in CDCl_3 at 25°C) for (a) $\text{V}(\text{NAd})\text{Me}_2[2-(2,6\text{-Me}_2\text{C}_6\text{H}_3)\text{NCH}_2-(\text{C}_5\text{H}_4\text{N})]$ (**2a**) and (b) **2a** with 1.0 equiv of $[\text{Ph}_3\text{C}][\text{B}(\text{C}_6\text{F}_5)_4]$ (in Et_2O , resultant reaction mixture after washing with *n*-hexane). ^1H NMR spectra (expanded between 1.3 and 2.4 ppm, in CDCl_3 at 25°C) for (c) $\text{V}(\text{NAd})\text{Me}_2[2-(2,6\text{-Me}_2\text{C}_6\text{H}_3)\text{NCH}_2-(\text{C}_5\text{H}_4\text{N})]$ (**2a**) and (d) **2a** with 1.0 equiv of $[\text{Ph}_3\text{C}][\text{B}(\text{C}_6\text{F}_5)_4]$ (in Et_2O , resultant reaction mixture after washing with *n*-hexane). More NMR data are shown in the Supporting Information.³¹

Table 2. Reaction with Ethylene by $\text{V}(\text{NAd})\text{X}_2[2-(2,6\text{-Me}_2\text{C}_6\text{H}_3)\text{NCH}_2-(\text{C}_5\text{H}_4\text{N})]$ [$\text{X} = \text{Cl}$ (**1**), Me (**2a**)]–Cocatalyst Systems^a

run	cat. (μmol)	Al cocat.	molar ratio ^b	oligomer				PE activity ^c
				activity ^c	TOF ^d	C_4' (%) ^e	C_6' (%) ^e	
1 ^f	1 (0.5)	MAO	500	50100	1830000	92.5	7.5	
2 ^f	1 (0.5)	MAO	500	50300	1800000	90.4	9.6	
3 ^f	1 (0.1)	MAO	1500	76500	2730000	97	3.0	
4 ^f	1 (5.0)	Me_2AlCl	200	trace				704 ^g
5 ^f	1 (5.0)	Et_2AlCl	100	trace				137 ^g
6	2a (0.5)	MAO	500	98800	3460000	91.0	9.0	
7	2a (0.5)	MAO	1500	82300	2880000	87.9	12.1	
8	2a (0.2)	MAO	1000	20700	725000	98.3	1.7	
9	2a (0.2)	MAO	1500	43600	1530000	97.1	2.9	
10	2a (0.2)	MAO	1500	35700	1250000	98.0	2.0	
11	2a (0.2)	MAO	2000	31900	1120000	98.4	1.6	
12	2a (2.0)	$\text{Al}^i\text{Bu}_3/\text{B}$	100/1.5	446	15600	>99	trace	42 ^h
13	2a (2.0)	$\text{Al}^i\text{Bu}_3/\text{B}$	200/1.5	128	4500	>99	trace	67 ^h

^aConditions: ethylene 8 atm, toluene 30 mL, *d*-MAO white solid (methylaluminoxane prepared by removing AlMe_3 , toluene from PMAO-S), 25°C (0°C , runs 4 and 5), 10 min (run 2, 20 min). ^bAl/V molar ratio. ^cActivity in kg ethylene reacted/mol V·h. ^dTOF (turnover frequency) = (molar amount of ethylene reacted)/(mol V·h). ^eBy GC analysis vs internal standard. ^fCited from our previous reports.^{12a,b} ^g $M_n = 5.92 \times 10^6$ (run 4); 6.76×10^6 (run 5). Samples were insoluble in ordinary GPC analysis in *o*-dichlorobenzene (at 145°C); molecular weight by viscosity.^{12b} ^hSamples were insoluble in ordinary GPC analysis in *o*-dichlorobenzene (at 145°C).

results clearly indicate that **2a** is an efficient catalyst for ethylene dimerization, and the catalyst performance (activity, selectivity) in **2a** was analogous to that in **1** under the same conditions.

However, the reactions in the presence of $[\text{Ph}_3\text{C}][\text{B}(\text{C}_6\text{F}_5)_4]$ and Al^iBu_3 afforded 1-butene and small amount of polyethylene that were insoluble for ordinary GPC measurements (in *o*-dichlorobenzene at 145°C). Although we do not have clear explanations for the observed results, these might be probably speculated as due to a catalyst/cocatalyst nuclearity effect, as shown in Scheme 2,^{12b,13b,c,14e,15} and we may consider that these might be due to a degree of (contact) interaction between the cationic alkyl species and the counteranion.

NMR Spectra of $\text{V}(\text{NAd})\text{X}_2[2\text{-ArNCH}_2(\text{C}_5\text{H}_4\text{N})]$ [$\text{X} = \text{Cl}$ (1**), Me (**2a**)] in Toluene- d_8 in the Presence of Al Cocatalysts.** We previously reported that ^{51}V NMR spectra

of a C_6D_6 solution containing the dichloro complex (**1**) in the presence of 10.0 equiv of MMAO (modified MAO, methyl isobutyl aluminoxane, at 25°C) showed a resonance at 32 ppm in addition to the resonance ascribed to **1** (-114 ppm), and the C_6D_6 solution in the presence of 10.0 equiv of Et_2AlCl showed another resonance (at -76 ppm, 25°C).^{12b,34} In contrast, no resonances were observed when $\text{V}(\text{NAd})\text{Cl}_3$ ³⁵ was treated with 10.0 equiv of Et_2AlCl under the same concentration (in C_6D_6 at 25°C).^{12b} Moreover, no resonances ascribed to formation of paramagnetic species were observed in the ESR measurement of the toluene solution of **1** upon addition of 100 equiv of MMAO, Et_2AlCl , whereas resonances ascribed to a paramagnetic species [vanadium(IV) species]^{17,18} were observed in the toluene solution containing $\text{V}(\text{NAd})\text{Cl}_3$ upon treatment with Et_2AlCl .^{12b} These results would support our hypothesis that the anionic ancillary donor ligand, (2-anilidomethyl)-

pyridine ligand, plays an essential role for stabilization of the oxidation state in this catalysis even in the presence of Al alkyls. Since the dimethyl complex (**2a**) exhibited catalyst performance similar to that of **1**, we measured NMR spectra in toluene- d_8 (solvent for the reaction) upon presence of Al cocatalysts.

Figure 3 shows ^{51}V NMR spectra of toluene- d_8 solution containing the dichloride complex (**1**) or dimethyl complex

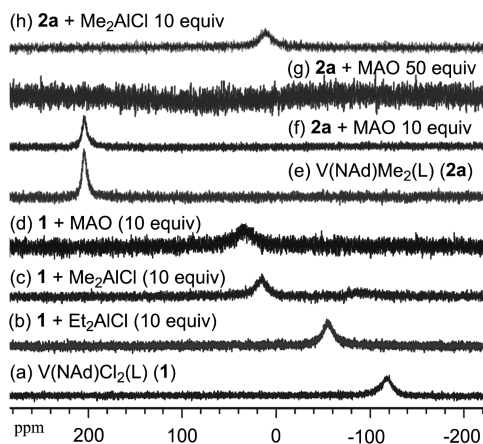


Figure 3. ^{51}V NMR spectra (in toluene- d_8 at 25 °C) for (a–d) $\text{V}(\text{NAd})\text{Cl}_2[2-(2,6\text{-Me}_2\text{C}_6\text{H}_3)\text{NCH}_2(\text{C}_5\text{H}_4\text{N})]$ (**1**) upon addition of Al cocatalyst (10.0 equiv) and (e–h) $\text{V}(\text{NAd})\text{Me}_2[2-(2,6\text{-Me}_2\text{C}_6\text{H}_3)\text{NCH}_2(\text{C}_5\text{H}_4\text{N})]$ (**2a**) upon addition of Al cocatalyst (10.0 or 50.0 equiv). More NMR data are shown in the Supporting Information.³⁴

(**2a**) in the presence of 10.0 equiv of MAO, Et_2AlCl , or Me_2AlCl (at 25 °C).³⁴ A new resonance at 36.1 ppm was observed when **1** (–120.6 ppm) was treated with MAO (10.0 equiv) with slightly decrease in the peak intensity (Figure 3d), suggesting formation of different vanadium(V) species from **1**. The other resonances, slightly shifted to high magnetic field side (–54.2, 14.7 ppm, respectively), were observed if **1** was treated with 10.0 equiv of Et_2AlCl or Me_2AlCl in toluene- d_8 at 25 °C (Figure 3b,c); significant decreases in the intensities in the spectra were not observed when these spectra were measured under the same vanadium concentrations (Figures 3a–c). Similar results were observed when these reactions (with MAO, Me_2AlCl , etc.) were conducted in C_6D_6 (data are shown in Figure S2-1).^{12b,34} Moreover, a resonance at 11.1

ppm was observed if the dimethyl complex (**2a**) was treated with Me_2AlCl (10.0 equiv) in toluene- d_8 (Figure 3h), and the resonance is close to that prepared by **1** with Me_2AlCl (Figure 3c). However, the spectrum of **2a** treated by 10.0 equiv of MAO showed the original resonance of **2a** with low intensity (Figures 3e–f); the resonance seems to almost have disappeared if **2a** was treated with 50.0 equiv of MAO (Figure 3g). This is because the solution consisted of two phases (toluene- d_8 soluble/insoluble), and the spectra of the soluble portion clearly showed only a resonance ascribed to the dimethyl complex (**2a**). The results are highly analogous to that observed in the reaction of **2a** with $[\text{Ph}_3\text{C}][\text{B}(\text{C}_6\text{F}_5)_4]$ in toluene- d_8 , and it seems likely that this would be due to a formation of the cationic species, although we have no clear explanations of observed difference between **1** and **2a** in the presence of MAO.

In contrast, no resonances were observed when $\text{V}(\text{NAd})\text{Cl}_3$ was treated with 10.0 equiv of Me_2AlCl in toluene- d_8 at 25 °C (homogeneous solution, data shown in the Figure S2-2),³⁴ as observed in the reaction of $\text{V}(\text{NAd})\text{Cl}_3$ with Et_2AlCl (10.0 equiv) in C_6D_6 .^{12b} As described above,^{12b} no resonances ascribed to formation of paramagnetic species were observed in the ESR measurement of the toluene solution of **1** upon addition of 100 equiv of MMAO, Et_2AlCl , whereas resonances ascribed to paramagnetic species [vanadium(IV) species] were observed in the toluene solution containing $\text{V}(\text{NAd})\text{Cl}_3$ upon treated with Et_2AlCl .^{12b} Therefore, these results could suggest that the chelate donor ligand, (2-anilidomethyl)pyridine ligand, plays an important role for stabilization of an oxidation state even in the presence of Al cocatalysts (MAO, Me_2AlCl , Et_2AlCl) in toluene. In addition to results in reactions of the dimethyl complex (**2a**) with borates, as described above, it thus seems highly likely that the cationic alkyl complex, $[\text{V}(\text{NAd})\text{Me}\{2\text{-ArNCH}_2(\text{C}_5\text{H}_4\text{N})\}]^+$, would play an important role in this catalysis.

Analysis of Catalyst Solution Consisting of $\text{V}(\text{NAd})\text{X}_2[2\text{-ArNCH}_2(\text{C}_5\text{H}_4\text{N})]$ [$\text{X} = \text{Cl}$ (1**), Me (**2a**)] and Al Cocatalysts in Toluene by Solution-Phase X-ray Absorption Spectroscopy.** As described above, on the basis of results in the NMR spectra of solutions prepared by **1** or **2a** with Al cocatalysts (and ESR data reported previously^{12b} by **1**) in toluene, we could demonstrate that the chelate anionic donor ligand plays a key role to stabilize the oxidation state of the

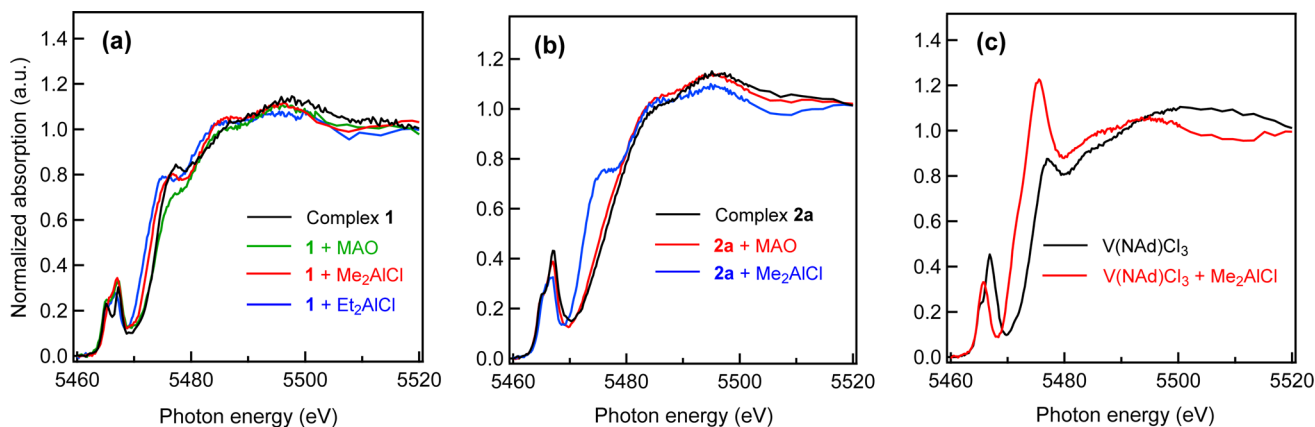


Figure 4. Solution-phase V K-edge XANES spectra (in toluene at 25 °C) for (a) $\text{V}(\text{NAd})\text{Cl}_2[2-(2,6\text{-Me}_2\text{C}_6\text{H}_3)\text{NCH}_2(\text{C}_5\text{H}_4\text{N})]$ (**1**) in the presence of Al cocatalyst (10.0 equiv), (b) $\text{V}(\text{NAd})\text{Me}_2[2-(2,6\text{-Me}_2\text{C}_6\text{H}_3)\text{NCH}_2(\text{C}_5\text{H}_4\text{N})]$ (**2a**) in the presence of Al cocatalyst (10.0 equiv), and (c) $\text{V}(\text{NAd})\text{Cl}_3$ and the solution upon addition of Me_2AlCl (10.0 equiv).³⁶

species formed *in situ*. These results, in addition to that in the reaction of **2a** with borate, would suggest a possibility that the cationic alkyl species would play a role in these catalysis. However, we could not totally exclude the other possibilities in vanadium catalysis. One probable reason we should take into consideration is that we could not completely exclude possibilities of formation of vanadium(III) and/or antiferromagnetically coupled vanadium(IV) dimer (ESR silent) under these experimental conditions.

Therefore, we focus on a possibility of synchrotron X-ray absorption spectroscopy (XAS) to explore obtainment of some structural information concerning the prepared catalyst solutions. In particular, the method (V–K edge analysis, 5.46 keV, through the use of synchrotron radiation at SPring-8, BL01B1 beamline) enables us to obtain information concerning oxidation state (by V–K pre-edge and edge peaks in XANES analysis, XANES = X-ray absorption near edge structure) as well as coordination atoms around the vanadium (by FT-EXAFS analysis, EXAFS = extended X-ray absorption fine structure).³⁶

Figure 4a shows solution-phase V K-edge XANES spectra of toluene solution containing the dichloride complex (**1**) in the presence of MAO, Me₂AlCl, and Et₂AlCl (10.0 equiv), and Figure 4b shows the spectra of toluene solution containing the dimethyl complex (**2a**) in the presence of MAO, Me₂AlCl (10.0 equiv). The spectra of the trichloride complex, V(NAd)Cl₃, and the solution in the presence of Me₂AlCl (10.0 equiv) are also shown in Figure 4c for comparison. The corresponding EXAFS spectrum of the dichloride complex (**1**) and the spectrum in the presence of MAO (10.0 equiv) are also shown in the Supporting Information.³⁶

The XANES spectrum of **1** shows pre-edge peaks at 5465.2 and 5467.3 eV, and the spectrum of **2a** shows the similar pre-edge peaks (5465.0 and 5467.1 eV), although **1** showed a shoulder-edge peak at 5477.8 eV. It turned out that the spectra (XANES and EXAFS) of **1** are good fittings of those based on both X-ray crystallographic analysis^{12a} and the DFT calculation (details are shown in the Supporting Information);³⁶ these suggest that solid-phase molecular geometries (trigonal bipyramidal geometry around V) were preserved in the solution phase. The curve-fitting of XANES spectrum of V(NAd)Cl₃ is also in good agreement with that estimated on the basis of DFT calculation (details are shown in the Supporting Information).³⁶ Two pre-edge peaks [observed at 5465.2 and 5467.3 eV (**1**), 5465.0 and 5467.1 eV (**2a**), and 5465.6 and 5467.1 eV in V(NAd)Cl₃] are generally considered as due to a transition from 1s to 3d + 4p,³⁷ although examples of solution V K-edge XANES spectra through the use of synchrotron radiation still have been limited.³⁸

Note that as shown in Figure 4a no significant differences in the XANES spectra (pre-edge peaks and edge) from that in **1** were observed upon addition of MAO [5465.1 and 5467.6 eV (pre-edge), 5477.8 eV (shoulder-edge)], Me₂AlCl [5465.6 and 5467.4 eV (pre-edge), 5476.4 eV (shoulder-edge)], and Et₂AlCl [5465.5 and 5466.8 eV (pre-edge), 5474.7 eV (shoulder-edge)], additional data are shown in the Figures S3-1–S3-3,³⁶ although intensity in a shoulder at the edge region (at 5477.8 eV) observed in **1** decreased upon addition of MAO.³⁹ Also note that the XANES spectrum of **1** in the presence of MAO is similar to those in the homogeneous toluene solution containing the dimethyl complex (**2a**) in the presence of MAO [5465.0 and 5467.0 eV (pre-edge)]⁴⁰ as well as that in **2a** itself [5465.0 and 5467.1 eV (pre-edge)], as shown in Figure

4b, although the spectrum of **1** in the presence of MAO showed a weak shoulder-edge peak at 5477.8 eV (might be corresponded to the residual **1**).^{39,40} Moreover, these results are reproducible (with different independent analysis runs, shown in the Figures S3-1 and S3-2).³⁶ Therefore, the results suggest in high certainty that similar catalytically active species were formed from **1** and **2a** upon addition of MAO, and the results would meet a good agreement with the fact that similar catalyst performances toward ethylene were observed between **1** and **2a** under the same conditions in the presence of MAO (Table 2).

Moreover, it should be noted that the spectrum of toluene solution of **1** in the presence of Me₂AlCl was very close to that of **2a** in the presence of Me₂AlCl (Figures 4a,b and S3-4).^{36,39} Since the results would also correspond to the fact that the ⁵¹V NMR spectra of toluene-*d*₈ solutions of **1** and **2a** in the presence of Me₂AlCl (10.0 equiv) showed similar resonances (Figure 3c,h), these results would also suggest a possibility that the similar species are formed in the (catalyst) solution. The spectrum of **1** in the presence of Et₂AlCl was similar to that of **1** in the presence of Me₂AlCl (Figure 4a); the results would also assume a possibility of formation of analogous species in the solution. Taking into account these XANES results in addition to the results in the ⁵¹V NMR spectra shown in Figure 3 (and our previous reported results that no paramagnetic species were formed from **1** upon addition of MMAO, Et₂AlCl in toluene),^{12b} it is thus clear that no significant changes in the oxidation state were observed from **1** and **2a** upon addition of Al cocatalysts (MAO, Me₂AlCl, Et₂AlCl) under conditions of reactions (dimerization or polymerization) conducted with ethylene shown in Table 2 (and reported previously with **1**).^{12a,b}

In contrast, certain significant changes in the XANES (pre-edge and edge region) spectrum were observed when the trichloride complex, V(NAd)Cl₃ [5465.6 and 5467.1 eV (pre-edge), 5476.7 eV (shoulder-edge)], was treated with Me₂AlCl [5465.8 eV (pre-edge), 5475.4 eV (shoulder-edge), Figure 4c].⁴¹ Since no resonances were observed when V(NAd)Cl₃ was treated with 10.0 equiv of Me₂AlCl in toluene-*d*₈ at 25 °C³⁴ and a similar result was observed in the reaction of V(NAd)Cl₃ with Et₂AlCl (10.0 equiv) in C₆D₆ [observed formation of paramagnetic species, V(IV), in the ESR measurement in the toluene solution^{12b}], the result would clearly suggest a formation of paramagnetic species. The results also strongly suggest that the chelate anionic donor ligand plays a role to stabilize the oxidation state upon addition of Al cocatalysts.

Moreover, no significant changes in both the EXAFS and the FT-EXAFS spectra were observed in toluene solutions of containing **1** upon addition of MAO (analysis data are shown in the Figure S3-8),³⁶ except that the apparent decrease in the intensity ascribed to V–Cl in **1** was observed upon addition of MAO.^{36,42} Note that at least two V–N σ -bonds (corresponding to vanadium–imido and –anilido) remained (observed) upon addition of MAO. These facts indicate that the coordinated Cl in **1** was removed by reaction with MAO without any changes for V–N bonds.⁴² Although more detailed analyses of EXAFS spectra in addition to XANES spectra are still in progress, we can at least say that the basic structure consisting of both imido and chelate anionic donor ligand would be preserved from **1** upon addition of MAO.⁴²

Taking into account both solution-phase V K-edge XANES and EXAFS data (and ⁵¹V NMR spectra shown in Figure 3, etc.), it is thus proposed that no significant changes in oxidation

of the catalyst solution consisting of **1** or **2a** and MAO and the formed vanadium(V) species retains the basic structure consisting of both imido and chelate anionic donor ligand; it thus seems highly likely that cationic alkyl species play a role in this catalysis.

CONCLUDING REMARKS

We have shown that the dimethyl complex, $V(\text{NAd})\text{Me}_2[2\text{-ArNCH}_2(\text{C}_5\text{H}_4\text{N})]$ (**2a**, Ar = 2,6-Me₂C₆H₃), prepared from the dichloro complex by treatment with LiMe, exhibited remarkable catalytic activity for ethylene dimerization in the presence of MAO [TOF = 1 120 000–1 530 000 h⁻¹ (311–425 s⁻¹), C₄' = 97.1–98.4%], and the catalyst performance was analogous to that of the dichloro analogue (**1**) under the same conditions. Reactions of **2a** with 1.0 equiv of R'OH afforded the corresponding mono alkoxide analogues, $V(\text{NAd})\text{Me}(\text{OR}')[2\text{-ArNCH}_2(\text{C}_5\text{H}_4\text{N})]$ [R' = C(CF₃)₃ (**3a**), C(CH₃)(CF₃)₂ (**3b**), C(CH₃)₃ (**3c**)], in high yields and structures of complexes **2a**, **3a–c** were determined by X-ray crystallography. The reaction of **2a** with 1.0 equiv of [Ph₃C][B(C₆F₅)₄] in Et₂O suggested formation of a cationic complex, $[V(\text{NAd})\text{Me}\{2\text{-ArNCH}_2(\text{C}_5\text{H}_4\text{N})\}]^+$, on the basis of ¹H, ¹⁹F, and ⁵¹V NMR spectra (Figure 2). Formation of another cationic species, $[V(\text{NAd})(\text{O}^t\text{Bu})\{2\text{-ArNCH}_2(\text{C}_5\text{H}_4\text{N})\}]^+$, was also observed in the NMR spectra when **3c** was treated with B(C₆F₅)₃ in THF.

On the basis of ⁵¹V NMR spectra of **1** and **2a** in the presence of Al cocatalysts (in toluene-*d*₈, Figure 3, and the data in C₆D₆ shown in the Supporting Information), in addition to our ESR data reported previously,^{12b} it was demonstrated that a chelate anionic (2-anilidomethyl)pyridine ligand plays a role to stabilize the oxidation state in this catalysis; these results thus suggest a possibility that the cationic alkyl complex, $[V(\text{NAd})\text{Me}\{2\text{-ArNCH}_2(\text{C}_5\text{H}_4\text{N})\}]^+$, would play an important role in this catalysis. This hypothesis was further explored by solution-phase V K-edge XAS analysis that showed no significant changes in the oxidation states were observed in the XANES spectra of **1** and **2a** in the presence of Al cocatalysts; the FT-EXAFS data also suggest a possibility that both the imido and the (2-anilidomethyl)pyridine ligands remained in the catalyst solution. The XAS analysis data could also exclude a possibility of formation of vanadium(III) species (ESR silent) *in situ*. Taking into account these results, it could be demonstrated with high certainty that the cationic vanadium(V) species play a role in this catalysis.

We believe that the results of this study introduce an important information for better understanding concerning a catalytically active species, especially with vanadium, as well as basic organometallic chemistry for the better catalyst design. Moreover, we also believe that combination of all analyses (NMR spectra, ESR spectra, and XAS analysis) and reaction chemistry would be helpful for providing more clear information for the better understanding. We are now exploring the more details including further analyses of the catalyst solutions (and complexes) through solution XAS (XANES, EXAFS) analysis including assignments of resonances; these would be introduced in the future.

EXPERIMENTAL SECTION

General Procedure. All experiments were carried out under a nitrogen atmosphere in a vacuum atmospheres drybox. Anhydrous-grade toluene and *n*-hexane (Kanto Kagaku Co., Ltd.) were transferred into a bottle containing molecular sieves (a mixture of 3A 1/16, 4A 1/8, and 13X 1/16) in the drybox under nitrogen stream, and were

passed through an alumina short column under N₂ stream prior to use. $V(\text{NAd})\text{Cl}_3$ ³⁵ and $V(\text{NAd})\text{Cl}_2[2\text{-}(2,6\text{-Me}_2\text{C}_6\text{H}_3)\text{NCH}_2(\text{C}_5\text{H}_4\text{N})]$ (**1**)^{12a} were prepared according to a published method. [Ph₃C][B(C₆F₅)₄] (Asahi Glass Co. Ltd.) were stored in the drybox and were used as received.

Elemental analyses were performed by using EAI CE-440 CHN/O/S Elemental Analyzer (Exeter Analytical, Inc.). All ¹H, ¹³C, ¹⁹F, and ⁵¹V NMR spectra were recorded on a Bruker AV500 spectrometer (500.13 MHz for ¹H, 125.77 MHz for ¹³C and 131.55 MHz for ⁵¹V). All spectra were obtained in the solvent indicated at 25 °C unless otherwise noted. Chemical shifts are given in ppm and are referenced to SiMe₄ (δ 0.00 ppm, ¹H, ¹³C), CFC₃ (δ 0.00 ppm, ¹⁹F), and VOCl₃ (δ 0.00 ppm, ⁵¹V). Coupling constants and half-width values, Δν_{1/2}, are given in Hz.

Synthesis of $V(\text{NAd})\text{Me}_2[2\text{-}(2,6\text{-Me}_2\text{C}_6\text{H}_3)\text{NCH}_2(\text{C}_5\text{H}_4\text{N})]$ (2a**).** Into a toluene (30 mL) and Et₂O (30 mL) solution containing $V(\text{NAd})\text{Cl}_2[2\text{-}(2,6\text{-Me}_2\text{C}_6\text{H}_3)\text{NCH}_2(\text{C}_5\text{H}_4\text{N})]$ (675 mg, 1.40 mmol) was added methyl lithium (2.80 mmol, Et₂O solution) at -30 °C. The reaction mixture was covered by aluminum foil to block out light and was warmed slowly to room temperature. The mixture was then stirred overnight. The solution was passed through a Celite pad, and the filter cake was washed with hot toluene. The combined filtrate and wash was placed in a rotary evaporator to remove the volatiles. The resultant solid was dissolved in a minimum amount of toluene, and was layered with *n*-hexane. The chilled solution placed in the freezer (-30 °C) afforded yellow crystals (480 mg, 1.12 mmol). Yield: 80.2%. ¹H NMR (C₆D₆, δ) 8.54 (d, 1H, J = 5.35 Hz, Py-H), 7.09 (d, 2H, J = 7.55 Hz, Ar-H), 7.01–6.95 (m, 2H, Ar-H and Py-H), 6.70 (t, 1H, J = 6.47 Hz, Py-H), 6.61 (d, 1H, J = 7.85 Hz, Py-H), 4.44 (s, 2H, NCH₂), 2.17 (s, 6H, Ar-CH₃), 2.07 (d, 6H, J = 2.55 Hz, Ad-H), 1.96 (brs, 3H, Ad-H), 1.58 (d, 3H, J = 11.80 Hz, Ad-H), 1.51 (d, 3H, J = 11.80 Hz, Ad-H), 0.92 (brs, 6H, VCH₃). ¹³C NMR (C₆D₆, δ) 161.8, 161.2, 147.9, 136.2, 132.0, 128.4, 124.4, 122.6, 120.3, 65.5, 43.5, 36.7, 29.9, 18.7. ⁵¹V NMR (C₆D₆, δ) 203.1 (Δν_{1/2} = 829 Hz). Anal. Calcd for C₂₆H₃₆N₃V: C, 70.73; H, 8.22; N, 9.52. Found: C, 71.09; H, 8.35; N, 9.29.

Synthesis of $V(\text{NAd})(\text{CH}_2\text{SiMe}_3)_2[2\text{-}(2,6\text{-Me}_2\text{C}_6\text{H}_3)\text{NCH}_2(\text{C}_5\text{H}_4\text{N})]$ (2b**).** Into a toluene solution (35 mL) containing $V(\text{NAd})\text{Cl}_2[2\text{-}(2,6\text{-Me}_2\text{C}_6\text{H}_3)\text{NCH}_2(\text{C}_5\text{H}_4\text{N})]$ (462 mg, 0.958 mmol) was added toluene solution (10 mL) containing LiCH₂SiMe₃ (180 mg, 1.92 mmol) at -30 °C. The reaction mixture was warmed slowly to room temperature, and the mixture was then stirred overnight. The solvent was removed *in vacuo*, and the resultant residue was extracted with *n*-hexane. The solution was passed through a Celite pad, and the filter cake was washed with *n*-hexane. The combined filtrate and wash was placed in a rotary evaporator to remove the volatiles. The resultant residue was dissolved in minimum amount of *n*-hexane, and yellow crystals (420 mg, 0.717 mmol) were obtained at -30 °C. Yield: 74.8%. ¹H NMR (C₆D₆, δ) 9.01 (d, 1H, J = 5.35 Hz, Py-H), 7.06 (d, 2H, J = 7.60 Hz, Ar-H), 7.03–6.97 (m, 2H, Ar-H and Py-H), 6.78 (t, 1H, J = 6.15 Hz, Py-H), 6.65 (d, 1H, J = 7.90 Hz, Py-H), 4.47 (s, 2H, NCH₂), 2.57 (d, 2H, J = 9.45 Hz, VCH₂), 2.18 (s, 6H, ArCH₃), 2.09 (d, 6H, J = 2.20 Hz, Ad-H), 1.97 (brs, 3H, Ad-H), 1.60 (d, 3H, J = 11.50 Hz, Ad-H), 1.50 (d, 3H, J = 11.80 Hz, Ad-H), 0.79 (d, 2H, J = 9.45 Hz, VCH₂), 0.12 (s, 18H, SiCH₃). ¹³C NMR (C₆D₆, δ) 162.7, 161.8, 148.0, 136.6, 132.2, 128.5, 124.7, 122.4, 120.6, 66.4, 43.4, 36.7, 29.9, 19.7, 3.4. ⁵¹V NMR (C₆D₆, δ) 244.4 (Δν_{1/2} = 1012 Hz). Anal. Calcd for C₃₂H₅₂N₃Si₂V: C, 65.60; H, 8.95; N, 7.17. Found: C, 65.73; H, 9.15; N, 7.05.

Synthesis of $V(\text{NAd})\text{Me}[\text{OC}(\text{CF}_3)_3][2\text{-}(2,6\text{-Me}_2\text{C}_6\text{H}_3)\text{NCH}_2(\text{C}_5\text{H}_4\text{N})]$ (3a**).** Into a toluene solution containing $V(\text{NAd})\text{Me}_2[2\text{-}(2,6\text{-Me}_2\text{C}_6\text{H}_3)\text{NCH}_2(\text{C}_5\text{H}_4\text{N})]$ (100 mg, 0.23 mmol) was added (CF₃)₃COH (67 mg, 0.28 mmol) at -30 °C. The reaction mixture was warmed slowly to room temperature, and the mixture was then stirred overnight. The reaction mixture was placed in a rotary evaporator to remove the volatiles. The residue was dissolved in a minimum amount of *n*-hexane. The chilled solution placed in the freezer (-30 °C) afforded yellow crystals (76 mg, 0.11 mmol). Yield: 50%. ¹H NMR (C₆D₆, δ) 8.61 (d, 1H, J = 5.05 Hz, Py-H), 7.06 (br, 1H, Ar-H), 6.99 (br, 2H, Ar-H), 6.92 (t, 1H, J = 7.58 Hz, Py-H),

Table 3. Crystal Data and Collection Parameters of V(NAd)Me₂[2-(2,6-Me₂C₆H₃)NCH₂(C₅H₄N)] (2), V(NAd)Me(OR)[2-(2,6-Me₂C₆H₃)NCH₂(C₅H₄N)] [R = C(CF₃)₃ (3a), C(CH₃)(CF₃)₂ (3b), and C(CH₃)₃ (3c)]^a

	2	3a	3b	3c
formula	C ₂₆ H ₃₆ N ₃ V	C ₂₉ H ₃₃ F ₉ N ₃ OV	C ₂₉ H ₃₆ F ₆ N ₃ OV	C ₂₉ H ₄₂ N ₃ OV
formula weight	441.53	661.53	607.55	499.61
crystal color, habit	yellow, acicular	yellow, block	yellow, block	orange, block
crystal size (mm)	0.360 × 0.230 × 0.180	0.330 × 0.290 × 0.180	0.241 × 0.208 × 0.200	0.310 × 0.250 × 0.230
crystal system	monoclinic	triclinic	triclinic	monoclinic
space group	P2 ₁ /c (#14)	P $\bar{1}$ (#2)	P $\bar{1}$ (#2)	P2 ₁ /n (#14)
a (Å)	18.88(2)	9.0936(7)	9.709(6)	10.439(7)
b (Å)	14.196(13)	11.9514(6)	9.814(6)	15.275(10)
c (Å)	20.00(2)	14.1528(12)	16.630(10)	17.444(11)
α (deg)		82.667(10)	73.62(2)	
β (deg)	116.71(2)	86.963(12)	73.71(2)	97.308(7)
γ (deg)		75.467(10)	78.33(3)	
V (Å ³)	4789(8)	1476.4(2)	1446(2)	2759(3)
Z value	8	2	2	4
D _{calcd} (g/cm ³)	1.225	1.488	1.395	1.203
F ₀₀₀	1888.00	680.00	632.00	1072.00
temp (K)	93	93	93	93
μ (Mo Kα) (cm ⁻¹)	4.309	4.209	4.086	3.842
no. of reflections measured (R _{int})	49795	15411	15304	28471
2θ _{max} (deg)	55.1	55.0	55.0	55.0
no. of observations [I > 2.00 σ(I)]	10970	6734	6604	6293
no. of variables	980	388	361	307
R ₁ [I > 2.00 σ(I)]	0.0575	0.0474	0.0487	0.0453
wR ₂ [I > 2.00 σ(I)]	0.1380	0.1364	0.1425	0.1615
goodness of fit	1.114	1.089	1.162	1.074

^aDetailed data are shown in the Supporting Information.²⁴

6.68 (t, 1H, J = 6.30 Hz, Py-H), 6.43 (d, 1H, J = 7.90 Hz, Py-H), 4.46 (d, 1H, J = 21.36 Hz, NCH₂), 4.20 (d, 1H, J = 21.36 Hz, NCH₂), 2.34 (s, 3H, ArCH₃), 2.00 (s, 3H, ArCH₃), 1.88–1.80 (m, 9H, Ad-H), 1.52 (s, 3H, VCH₃), 1.45–1.38 (m, 6H, Ad-H). ¹³C NMR (C₆D₆, δ) 162.4, 159.1, 148.2, 137.0, 131.9, 130.9, 128.3, 128.5, 128.2, 127.9, 125.4, 123.7, 122.4, 121.3, 119.6, 67.6, 42.1, 36.3, 29.7, 18.2, 18.1. ¹⁹F NMR (C₆D₆, δ) -73.7. ⁵¹V NMR (C₆D₆, δ) -112.1 (Δν_{1/2} = 1160 Hz).

Synthesis of V(NAd)Me[OC(CF₃)₂(CH₃)] [2-(2,6-Me₂C₆H₃)-NCH₂(C₅H₄N)] (3b). Into a toluene solution containing V(NAd)-Me₂[2-(2,6-Me₂C₆H₃)NCH₂(C₅H₄N)] (110 mg, 0.26 mmol) was added (CH₃)(CF₃)₂COH (80 mg, 0.44 mmol) at -30 °C. The reaction mixture was warmed slowly to room temperature, and the mixture was then stirred overnight. The reaction mixture was placed in a rotary evaporator to remove the volatiles. The residue was dissolved in a minimum amount of *n*-hexane. The chilled solution placed in the freezer (-30 °C) afforded yellow crystals (101 mg, 0.166 mmol). Yield: 65%. ¹H NMR (C₆D₆, δ) 8.82 (d, 1H, J = 5.35 Hz, Py-H), 7.08–6.98 (m, 3H, Ar-H), 6.90 (t, 1H, J = 7.57 Hz, Py-H), 6.70 (t, 1H, J = 6.30 Hz, Py-H), 6.42 (d, 1H, J = 7.85 Hz, Py-H), 4.37 (d, 1H, J = 21.13 Hz, NCH₂), 4.29 (d, 1H, J = 21.13 Hz, NCH₂), 2.28 (s, 3H, ArCH₃), 2.11 (s, 3H, OC(CH₃)), 1.93 (s, 3H, ArCH₃), 1.82 (brs, 3H, Ad-H), 1.80 (brs, 6H, Ad-H), 1.41 (brs, 6H, Ad-H), 1.37 (s, 3H, VCH₃). ¹⁹F NMR (C₆D₆, δ) -78.1 (q, J = 8.66 Hz), -78.9 (q, J = 8.66 Hz). ⁵¹V NMR (C₆D₆, δ) -161.1 (Δν_{1/2} = 1118 Hz).

Synthesis of V(NAd)Me[OC(CH₃)₃] [2-(2,6-Me₂C₆H₃)-NCH₂(C₅H₄N)] (3c). Into a toluene solution containing V(NAd)-Me₂[2-(2,6-Me₂C₆H₃)NCH₂(C₅H₄N)] (200 mg, 0.45 mmol) was added ⁴BuOH (40 mg, 0.54 mmol) at -30 °C. The reaction mixture was warmed slowly to room temperature, and the mixture was then stirred overnight. The reaction mixture was placed in a rotary evaporator to remove the volatiles. The resultant residue was dissolved in a minimum amount of *n*-hexane, and yellow solids (132 mg, 0.264 mmol) were obtained at -30 °C. Yield: 58%. ¹H NMR (CDCl₃, δ) 8.84 (d, 1H, J = 5.05 Hz, Py-H), 7.76 (td, 1H, J = 7.56, 1.58 Hz, Py-H), 7.36 (t, 1H, J = 6.32 Hz, Py-H), 7.27 (d, 1H, Py-H, overlapping

with solvent), 7.05 (d, 2H, J = 7.55 Hz, Ar-H), 6.93 (t, 1H, J = 7.55 Hz, Ar-H), 4.75 (d, 1H, J = 20.81 Hz, NCH₂), 4.68 (d, 1H, J = 20.81 Hz, NCH₂), 2.20 (s, 3H, ArCH₃), 2.19 (s, 3H, ArCH₃), 1.81 (brs, 3H, Ad-H), 1.62 (d, 6H, J = 2.55 Hz, Ad-H), 1.43 (d, 3H, J = 12.15 Hz, Ad-H), 1.38 (d, 3H, J = 12.15 Hz, Ad-H), 1.32 (s, 9H, C(CH₃)₃), 0.63 (s, 3H, VCH₃). ¹³C NMR (CDCl₃, δ) 160.4, 148.5, 136.2, 132.7, 132.0, 128.3, 128.0, 128.0, 123.7, 121.9, 119.2, 66.1 (NCH₂), 42.8, 36.2, 33.3, 29.4, 18.8 (ArCH₃), 18.2 (ArCH₃). ⁵¹V NMR (C₆D₆, δ) -246.5 (Δν_{1/2} = 687 Hz).

Reaction of V(NAd)Me₂[2-(2,6-Me₂C₆H₃)NCH₂(C₅H₄N)] (2a) with Borate. [Ph₃C][B(C₆F₅)₄] (209 mg, 0.227 mmol) was added to Et₂O (40 mL) containing V(NAd)Me₂[2-(2,6-Me₂C₆H₃)-NCH₂(C₅H₄N)] (100 mg, 0.226 mmol) at -30 °C. The solution was stirred 1 h at room temperature. After reaction, the solution was placed in a rotary evaporator to remove the solvent. The residue was dissolved in Et₂O and dropped into *n*-hexane. Removal of hexane layer and washing by hexane afforded the residue (265 mg). ¹H NMR ([solvent], δ) 8.41 (d, 1H, J = 5.35 Hz, Py-H), 8.12 (t, 1H, J = 7.73 Hz, Py-H), 7.70 (d, 1H, J = 8.15 Hz, Py-H), 7.64 (t, 1H, J = 6.48 Hz, Py-H), 7.25–7.09 (m, 3H, Ar-H), 5.26 (d, 1H, J = 22.71 Hz, NCH₂), 5.20 (d, 1H, J = 22.71 Hz, NCH₂), 4.04–3.89 (m, 4H, OCH₂), 2.27 (s, 3H, Ad-H), 1.94 (brs, 6H, ArCH₃), 1.69 (d, 3H, J = 12.45 Hz, Ad-H), 1.66 (d, 3H, J = 12.45 Hz, Ad-H), 1.53 (brs, 3H, VCH₃), 1.53–1.40 (m, 6H, Ad-H), 1.32 (t, 6H, J = 7.08 Hz, OCH₂CH₃). ¹⁹F NMR (CDCl₃, δ) -132.6 (brs), -163.0 (t, J = 20.3 Hz), -166.8 (brs). ⁵¹V NMR (CDCl₃, δ) 83.6 (Δν_{1/2} = 2763 Hz).

Reaction of V(NAd)Me[OC(CH₃)₃] [2-(2,6-Me₂C₆H₃)-NCH₂(C₅H₄N)] (3c) with B(C₆F₅)₃. B(C₆F₅)₃ (10 mg, 0.040 mmol) was added to THF (2 mL) containing V(NAd)Me(O^tBu)[2-(2,6-Me₂C₆H₃)NCH₂(C₅H₄N)] (20 mg, 0.040 mmol) at -30 °C. The solution was stirred 1 h at room temperature. After reaction, the solution was placed in a rotary evaporator to remove the solvent. The residue was dissolved in THF and dropped into *n*-hexane. Removal of *n*-hexane layer and washing by *n*-hexane afforded the residue (20 mg). ¹H NMR (CDCl₃, δ) 8.26 (d, 1H, J = 5.35 Hz, Py-H), 7.93 (td, 1H, J = 7.55, 1.25 Hz, Py-H), 7.48–7.43 (m, 2H, Py-H), 7.23 (t, 1H, J =

4.70 Hz, Ar-H), 7.14 (d, 2H, $J = 4.40$ Hz, Ar-H), 5.22 (d, 1H, $J = 22.08$ Hz, NCH₂), 5.04 (d, 1H, $J = 22.08$ Hz, NCH₂), 4.09 (br, 2H, coordinated THF), 3.99 (br, 2H, coordinated THF), 3.77 (br, 4H, free THF), 2.34 (s, 3H, Ad-H), 2.08 (s, 6H, ArCH₃), 1.88 (br, 8H, coordinated and free THF), 1.62–1.43 (m, 9H, Ad-H), 1.41 (s, 9H, ^tBu-H), 1.34–1.26 (m, 3H, Ad-H), 0.48 (brs, 3H, BCH₃). ¹⁹F NMR (CDCl₃, δ) -132.7 (d, $J = 20.8$ Hz), -164.7 (t, $J = 19.1$ Hz), -167.3 (dd, $J = 20.8, 19.1$ Hz). ⁵¹V NMR (CDCl₃, δ) -309.6 ($\Delta\nu_{1/2} = 1842$ Hz).

Crystallographic Analysis. All of measurements made on a Rigaku XtaLAB mini Imaging Plate diffractometer with graphite monochromated Mo $K\alpha$ radiation. The crystal collection parameters are listed below (Table 3). All structures were solved by direct methods and expanded using Fourier techniques, and the non-hydrogen atoms were refined anisotropically.⁴³ Hydrogen atoms were refined using the riding model. All calculations were performed using the Crystal Structure⁴⁴ crystallographic software package except for refinement, which was performed using SHELXL-97.⁴⁵ Details are shown in the Supporting Information.²⁴

Reaction with Ethylene. Ethylene oligomerizations were conducted in a 100 mL scale stainless-steel autoclave, and the typical reaction procedure is as follows. Toluene (29.0 mL) and the prescribed amount of MAO were added into the autoclave in the drybox. The reaction apparatus was then filled with ethylene (1 atm), and the prescribed amount of complex, V(NAd)Me₂[2-(2,6-Me₂C₆H₃)NCH₂(C₅H₄N)] (2a), in toluene (1.0 mL) was added into the autoclave. The reaction apparatus was then immediately pressurized to 7 atm (total 8 atm), and the mixture was magnetically stirred for 10 min (ethylene pressure was kept constant during the reaction). After the above procedure, the remaining ethylene was purged at -30 °C, and 0.5 g of *n*-heptane was added as an internal standard. The solution was then analyzed by GC to determine the activity and the product distribution. In the case of reaction in the presence of [Ph₃C][B(C₆F₅)₄], a toluene solution containing [Ph₃C][B(C₆F₅)₄] was added after injecting a toluene solution containing catalyst (2a). After the above oligomerization procedure, the remaining mixture in autoclave was poured into MeOH containing HCl, and the resultant polymer (white precipitate) was collected on a filter paper by filtration and was adequately washed with MeOH. The resultant polymer was then dried *in vacuo* at 60 °C for 2 h.

⁵¹V NMR Experiments in the Reaction of V(NAd)X₂[2-(2,6-Me₂C₆H₃)NCH₂(C₅H₄N)] [X = Cl (1), Me (2a)] with Al Cocatalysts in Toluene-*d*₈. Typical procedure is as follows. Into a toluene-*d*₈ solution (ca. 0.6 mL) containing 1 or 2a (25 μ mol, ca. 42 μ mol/mL) placed in the freezer (-30 °C) was added Al cocatalyst (MAO, Me₂AlCl, or Et₂AlCl; 250 μ mol, 10.0 equiv). The mixture was then measured by ⁵¹V NMR spectrum at 25 °C within 10 min after the preparation.

Analysis of Catalyst Solution by Solution-Phase X-ray Absorption Spectroscopy. V K-edge X-ray absorption fine structure (XAFS) measurements were carried out at the BL01B1 beamline at the SPring-8 facility of the Japan Synchrotron Radiation Research Institute (proposal nos. 2015B1308, 2016A1455). The measurements were conducted at room temperature. A Si (111) two-crystal monochromator was used for the incident beam. V K-edge XAFS spectra of V complex samples (prepared as toluene solution, 50 μ mol/mL) were recorded in the fluorescence mode using an ionization chamber as the I₀ detector and 19 solid-state detectors as the I detector. The X-ray energy was calibrated using V₂O₅. Data analysis was performed with the REX2000 ver. 2.5.9 software package (Rigaku Co.). The X-ray absorption near edge structure (XANES) data was analyzed by removing the atomic absorption background using a cubic spline from the χ spectra and normalization of them to the edge height. The extended X-ray absorption fine structure (EXAFS) data were analyzed as follows. The χ spectra were extracted by removing the atomic absorption background using a cubic spline and were normalized to the edge height. The k^3 -weighted χ spectra were Fourier transformed (FT) into the r space, using the FT range 3.0–12 Å⁻¹. The curve fitting range was 1.0–2.3 Å. The phase shift and backscattering amplitude functions of V–N and V–Cl bonds were

extracted from V(NAd)Cl₂[2-(2,6-Me₂C₆H₃)NCH₂(C₅H₄N)] (1) structure using FEFF8 ($\sigma^2 = 0.0036$ (σ : Debye–Waller factor)).

■ ASSOCIATED CONTENT

Supporting Information

The Supporting Information is available free of charge on the ACS Publications website at DOI: 10.1021/acs.organomet.6b00727.

NMR spectra in the reactions of V(NAd)Me₂[2-(2,6-Me₂C₆H₃)NCH₂(C₅H₄N)] (2a) with [Ph₃C][B(C₆F₅)₄], V(NAd)Me(O^{*t*}Bu)[2-(2,6-Me₂C₆H₃)NCH₂(C₅H₄N)] (3c) with B(C₆F₅)₃. Additional NMR spectra of C₆D₆ solution of V(NAd)Me₂[2-(2,6-Me₂C₆H₃)NCH₂(C₅H₄N)] (2a) in the presence of Al cocatalysts. Additional data including XANES and EXAFS spectra and curve fittings [for V(NAd)Cl₃, V(NAd)Cl₂[2-(2,6-Me₂C₆H₃)CH₂C₅H₄N] (1) by calculations on the basis of X-ray crystallographic structure and/or DFT calculations]. (PDF)

Crystallographic information file for V(NAd)Me₂[2-ArNCH₂(C₅H₄N)] (2a), V(NAd)Me(OR')[2-ArNCH₂(C₅H₄N)] [R' = OC(CF₃)₃ (3a), OC(CF₃)₂(CH₃) (3b), OC(CH₃)₃ (3c)] (CIF)

Cartesian coordinates for V(NAd)Me₂[2-ArNCH₂(C₅H₄N)] (2a), V(NAd)Me(OR')[2-ArNCH₂(C₅H₄N)] [R' = OC(CF₃)₃ (3a), OC(CF₃)₂(CH₃) (3b), OC(CH₃)₃ (3c)] (XYZ)

(PDF)

(CIF)

(XYZ)

■ AUTHOR INFORMATION

Corresponding Authors

*E-mail: ktnomura@tmu.ac.jp. Tel./Fax: +81-42-677-2547.

*E-mail: mitsudom@cheng.es.osaka-u.ac.jp.

*E-mail: takaya@sci.kyoto-u.ac.jp.

*E-mail: yamazoe@chem.s.u-tokyo.ac.jp.

ORCID

Kotohiro Nomura: 0000-0003-3661-6328

Notes

The authors declare no competing financial interest.

■ ACKNOWLEDGMENTS

This project was partly supported by Grant-in-Aid for Scientific Research on Innovative Areas ("3D Active-Site Science", No. 26105003) from The Ministry of Education, Culture, Sports, Science and Technology (MEXT). The synchrotron XAFS analysis were performed at SPring-8 beamlines of BL01B1 with the approval of JASRI (2015B1308, 2016A1455). A.I. expresses his thanks to JSPS for predoctoral fellowship (DC2 26-7313). The authors would also express their heartfelt thanks to Prof. Zen Maeno, Prof. Koichiro Jitsukawa, and Prof. Kiyotomi Kaneda (Osaka University) for their big supports for collaboration of XAFS analysis at SPring 8. K.N. expresses his thanks to Mr. Takumi Yamada, Mr. Shuta Ito, Mr. Tomohiro Miwata, and Dr. Shunsuke Sueki (Tokyo Metropolitan Univ., TMU) for helping measurement of synchrotron XAFS analysis at Spring 8, and to Prof. Masaharu Nakamura (Kyoto University), Profs. S. Komiya, A. Inagaki (TMU) for discussions.

REFERENCES

- (1) For example, see (a) Vogt, D. In *Applied Homogeneous Catalysis with Organometallic Compounds*; Cornils, B., Herrmann, W. A., Eds.; Wiley VCH: Weinheim, Germany, 2000; pp 245. (b) van Leeuwen, P. W. N. N. *Homogeneous Catalysis*; Kluwer Academic Publishers: Dordrecht, Germany, 2004; pp 175. (c) Steinborn, D. *Fundamentals of Organometallic Catalysis*; Wiley-VCH: Weinheim, Germany, 2012; pp 145.
- (2) (a) Peuckert, M.; Keim, W. *Organometallics* **1983**, *2*, 594. (b) Peuckert, M.; Keim, W.; Storp, S.; Weber, R. S. *J. Mol. Catal.* **1983**, *20*, 115. (c) Keim, W. *Angew. Chem., Int. Ed. Engl.* **1990**, *29*, 235. (d) Keim, W. *Angew. Chem., Int. Ed.* **2013**, *52*, 12492.
- (3) For review for metal catalyzed dimerization of ethylene, propylene, see (a) Pillai, S. M.; Ravindranathan, M.; Sivaram, S. *Chem. Rev.* **1986**, *86*, 353. (b) Skupinska, J. *Chem. Rev.* **1991**, *91*, 613. (c) Takeuchi, D.; Osakada, K. In *Organometallic Reactions and Polymerization*; Osakada, K., Ed.; Lecture Note in Chemistry 85; Springer-Verlag, Berlin, 2014; p 169.
- (4) For selected pioneering examples and recent reviews, see (a) Killian, C. M.; Johnson, L. K.; Brookhart, M. *Organometallics* **1997**, *16*, 2005. (b) Svejda, S. A.; Brookhart, M. *Organometallics* **1999**, *18*, 65. (c) Komon, Z. J. A.; Bu, X.; Bazan, G. C. *J. Am. Chem. Soc.* **2000**, *122*, 12379. (d) Speiser, F.; Braunstein, P.; Saussine, L. *Acc. Chem. Res.* **2005**, *38*, 784. (e) Wang, S.; Sun, W.-H.; Redshaw, C. *J. Organomet. Chem.* **2014**, *751*, 717.
- (5) For selected pioneering examples and recent reviews, see (a) Small, B. L.; Brookhart, M. *J. Am. Chem. Soc.* **1998**, *120*, 7143. (b) Britovsek, G. J. P.; Mastroianni, S.; Solan, G. A.; Baugh, S. P. D.; Redshaw, C.; Gibson, V. C.; White, A. J. P.; Williams, D. J.; Elsegood, M. R. *J. Chem. - Eur. J.* **2000**, *6*, 2221. (c) Zhang, W.; Sun, W.-H.; Redshaw, C. *Dalton Trans.* **2013**, *42*, 8988. (d) Boudier, A.; Breuil, P.-A. R.; Magna, L.; Olivier-Bourbigou, H.; Braunstein, P. *Chem. Commun.* **2014**, *50*, 1398. (e) Ma, J.; Feng, C.; Wang, S.; Zhao, K.; Sun, W.-H.; Redshaw, C.; Solan, G. A. *Inorg. Chem. Front.* **2014**, *1*, 14. (f) Small, B. L. *Acc. Chem. Res.* **2015**, *48*, 2599.
- (6) Reagan, W. K. Patent EP 0417477 B1, Phillips Petroleum Company, 1991.
- (7) For recent selected reviews, see (a) Dixon, J. T.; Green, M. J.; Hess, F. M.; Morgan, D. H. *J. Organomet. Chem.* **2004**, *689*, 3641. (b) McGuinness, D. S. *Chem. Rev.* **2011**, *111*, 2321. (c) Agapie, T. *Coord. Chem. Rev.* **2011**, *255*, 861. (d) van Leeuwen, P. W. N. M.; Clément, N. D.; Tschan, M. J.-L. *Coord. Chem. Rev.* **2011**, *255*, 1499. (e) McGuinness, D. S. In *Olefin Upgrading Catalysis by Nitrogen-based Metal Complexes*; Giambastiani, G., Cãmpora, J., Eds.; Catalysis by Metal Complexes 35; Springer Science +Business: Dordrecht, 2011; p 1. (f) Agapie, T. *Coord. Chem. Rev.* **2011**, *255*, 861.
- (8) For selected examples, see (a) Wass, D. F. *Dalton Trans.* **2007**, 816. (b) Tomov, A. K.; Chirinos, J. J.; Long, R. J.; Gibson, V. C.; Elsegood, M. R. *J. Am. Chem. Soc.* **2006**, *128*, 7704. (c) Brückner, A.; Jabor, J. K.; McConnell, A. E. C.; Webb, P. B. *Organometallics* **2008**, *27*, 3849. (d) McGuinness, D. S.; Suttill, J. A.; Gardiner, M. G.; Davies, N. W. *Organometallics* **2008**, *27*, 4238. (e) Zhang, J.; Braunstein, P.; Hor, T. S. A. *Organometallics* **2008**, *27*, 4277. (f) Hanton, M. J.; Tenza, K. *Organometallics* **2008**, *27*, 5712. (g) Kirillov, E.; Roisnel, T.; Razavi, A.; Carpentier, J.-F. *Organometallics* **2009**, *28*, 2401. (h) Zhang, J.; Li, A.; Hor, T. S. A. *Organometallics* **2009**, *28*, 2935. (i) Dulai, A.; de Bod, H.; Hanton, M. J.; Smith, D. M.; Downing, S.; Mansell, S. M.; Wass, D. F. *Organometallics* **2009**, *28*, 4613. (j) Tenza, K.; Hanton, M. J.; Slawin, A. M. Z. *Organometallics* **2009**, *28*, 4852. (k) Vidyaratne, I.; Nikiforov, G. B.; Gorelsky, S. I.; Gambarotta, S.; Duchateau, R.; Korobkov, I. *Angew. Chem., Int. Ed.* **2009**, *48*, 6552. (l) Klemp, C.; Payet, E.; Magna, L.; Saussine, L.; LeGoff, X. F.; Le Floch, P. *Chem. - Eur. J.* **2009**, *15*, 8259. (m) Peitz, S.; Peulecke, N.; Aluri, B. R.; Müller, B. H.; Spannenberg, A.; Rosenthal, U.; Al-Hazmi, M. H.; Mosa, F. M.; Wöhl, A.; Müller, W. *Organometallics* **2010**, *29*, 5263. (n) Licciulli, S.; Thapa, I.; Albahily, K.; Korobkov, I.; Gambarotta, S.; Duchateau, R.; Chevalier, R.; Schuhen, K. *Angew. Chem., Int. Ed.* **2010**, *49*, 9225. (o) Albahily, K.; Fomitcheva, V.; Gambarotta, S.; Korobkov, I.; Murugesu, M.; Gorelsky, S. I. *J. Am. Chem. Soc.* **2011**, *133*, 6380.
- (p) Albahily, K.; Shaikh, Y.; Sebastiao, E.; Gambarotta, S.; Korobkov, I.; Gorelsky, S. I. *J. Am. Chem. Soc.* **2011**, *133*, 6388. (q) Dulai, A.; McMullin, C. L.; Tenza, K.; Wass, D. F. *Organometallics* **2011**, *30*, 935. (r) Peitz, S.; Peulecke, N.; Müller, B. H.; Spannenberg, A.; Drexler, H.-J.; Rosenthal, U.; Al-Hazmi, M. H.; Al-Eidan, K. E.; Wöhl, A.; Müller, W. *Organometallics* **2011**, *30*, 2364. (s) Albahily, K.; Shaikh, Y.; Ahmed, Z.; Korobkov, I.; Gambarotta, S.; Duchateau, R. *Organometallics* **2011**, *30*, 4159. (t) Albahily, K.; Fomitcheva, V.; Shaikh, Y.; Sebastiao, E.; Gorelsky, S. I.; Gambarotta, S.; Korobkov, I.; Duchateau, R. *Organometallics* **2011**, *30*, 4201. (u) Albahily, K.; Gambarotta, S.; Duchateau, R. *Organometallics* **2011**, *30*, 4655. (v) Thapa, I.; Gambarotta, S.; Korobkov, I.; Murugesu, M.; Budzelaar, P. *Organometallics* **2012**, *31*, 486. (w) Sydora, O. L.; Jones, T. C.; Small, B. L.; Nett, A. J.; Fischer, A. A.; Carney, M. J. *ACS Catal.* **2012**, *2*, 2452. (x) Heinig, S.; Wöhl, A.; Müller, B. H.; Al-Hazmi, M. H.; Müller, B. H.; Peulecke, N.; Rosenthal, U. *ChemCatChem* **2013**, *5*, 3107. (y) Monillas, W. H.; Young, J. F.; Yap, G. P. A.; Theopold, K. H. *Dalton Trans.* **2013**, *42*, 9198.
- (9) For selected examples for Ti, Zr complex catalysts, see (a) Wielstra, Y.; Gambarotta, S.; Chiang, Y. *Organometallics* **1988**, *7*, 1866. (b) Deckers, P. J. W.; Hessen, B.; Teuben, J. H. *Angew. Chem., Int. Ed.* **2001**, *40*, 2516. (c) Deckers, P. J. W.; Hessen, B.; Teuben, J. H. *Organometallics* **2002**, *21*, 5122. (d) You, Y.; Girolami, G. S. *Organometallics* **2008**, *27*, 3172. (e) Otten, E.; Batinas, A. A.; Meetsma, A.; Hessen, B. *J. Am. Chem. Soc.* **2009**, *131*, 5298. (f) Suzuki, Y.; Kinoshita, S.; Shibahara, A.; Ishii, S.; Kawamura, K.; Inoue, Y.; Fujita, T. *Organometallics* **2010**, *29*, 2394. (g) Kinoshita, S.; Kawamura, K.; Fujita, T. *Chem. - Asian J.* **2011**, *6*, 284.
- (10) Ta catalysts; see (a) Fellmann, J. D.; Rupprecht, G. A.; Schrock, R. R. *J. Am. Chem. Soc.* **1979**, *101*, 5099. Ligand-free TaCl₅-cocatalyst systems were used in the refs 10b and 10c. (b) Andes, C.; Harkins, S. B.; Murtuza, S.; Oylar, K.; Sen, A. *J. Am. Chem. Soc.* **2001**, *123*, 7423. (c) Arteaga-Müller, R.; Tsurugi, H.; Saito, T.; Yanagawa, M.; Oda, S.; Mashima, K. *J. Am. Chem. Soc.* **2009**, *131*, 5370.
- (11) V complex catalysts, see ref 8f (a) Brussee, E. A. C.; Meetsma, A.; Hessen, B.; Teuben, J. H. *Chem. Commun.* **2000**, 497. (b) Schmidt, R.; Welch, M. B.; Knudsen, R. D.; Gottfried, S.; Alt, H. G. *J. Mol. Catal. A: Chem.* **2004**, *222*, 17. Vanadium complexes containing chelate bis(imino)pyridine ligands yielded polymers/oligomers with Schultz-Flory distribution.
- (12) (a) Zhang, S.; Nomura, K. *J. Am. Chem. Soc.* **2010**, *132*, 4960. (b) Igarashi, A.; Zhang, S.; Nomura, K. *Organometallics* **2012**, *31*, 3575. (c) Nomura, K.; Igarashi, A.; Katao, S.; Zhang, W. J.; Sun, W.-H. *Inorg. Chem.* **2013**, *52*, 2607. (d) Tang, X.-Y.; Igarashi, A.; Sun, W.-H.; Inagaki, A.; Liu, J.; Zhang, W.; Li, Y.-S.; Nomura, K. *Organometallics* **2014**, *33*, 1053.
- (13) (a) Nomura, K.; Sagara, A.; Imanishi, Y. *Macromolecules* **2002**, *35*, 1583. (b) Wang, W.; Nomura, K. *Macromolecules* **2005**, *38*, 5905. (c) Wang, W.; Nomura, K. *Adv. Synth. Catal.* **2006**, *348*, 743.
- (14) For recent reviews (vanadium catalysts), see (a) Hagen, H.; Boersma, J.; van Koten, G. *Chem. Soc. Rev.* **2002**, *31*, 357. (b) Gambarotta, S. *Coord. Chem. Rev.* **2003**, *237*, 229. (c) Nomura, K.; Zhang, W. *Chem. Sci.* **2010**, *1*, 161. (d) Redshaw, C. *Dalton Trans.* **2010**, *39*, 5595. (e) Nomura, K.; Zhang, S. *Chem. Rev.* **2011**, *111*, 2342. and related references cited therein.
- (15) (a) Macchioni, A. *Chem. Rev.* **2005**, *105*, 2039. (b) Li, H.; Marks, T. J. *Proc. Natl. Acad. Sci. U. S. A.* **2006**, *103*, 15295. (c) Bochmann, M. *Organometallics* **2010**, *29*, 4711. (d) Metal-metal cooperative effects in olefin polymerization: McInnis, J. P.; Delferro, M.; Marks, T. J. *Acc. Chem. Res.* **2014**, *47*, 2545.
- (16) Goswami, M.; Chirila, A.; Rebreyend, C.; de Bruin, B. *Top. Catal.* **2015**, *58*, 719.
- (17) Pioneering ESR study for monitoring the catalytically active species (VCl₄-Et₂AlCl catalyst system): Lehr, M. H.; Carman, C. J. *Macromolecules* **1969**, *2*, 217.
- (18) For selected recent examples for ESR study of vanadium species formed by treatment with Al alkyls, see: (a) Bigmore, H. B.; Zuidveld, M. A.; Kowalczyk, R. M.; Cowley, A. R.; Kranenburg, M.; McInnes, E. J. L.; Mountford, P. *Inorg. Chem.* **2006**, *45*, 6411. (b) Soshnikov, I. E.;

Semikolenova, N. V.; Bryliakov, K. P.; Zakharov, V. A.; Redshaw, C.; Talsi, E. P. *J. Mol. Catal. A: Chem.* **2009**, *303*, 23. (c) Soshnikov, I. E.; Semikolenova, N. V.; Shubin, A. A.; Bryliakov, K. P.; Zakharov, V. A.; Redshaw, C.; Talsi, E. P. *Organometallics* **2009**, *28*, 6714.

(19) (a) Carrick, W. L. *J. Am. Chem. Soc.* **1958**, *80*, 6455. (b) Carrick, W. L.; Kluijber, R. W.; Bonner, E. F.; Wartman, L. H.; Rugg, F. M.; Smith, J. J. *J. Am. Chem. Soc.* **1960**, *82*, 3883. (c) Phillips, G. W.; Carrick, W. L. *J. Polym. Sci.* **1962**, *59*, 401.

(20) (a) Junghanns, E.; Gumboldt, O.; Bier, G. *Makromol. Chem.* **1962**, *58*, 18. (b) Natta, G.; Mazzanti, G.; Valvassori, A.; Sartori, G.; Fiumani, D. *J. Polym. Sci.* **1961**, *51*, 411.

(21) For example: Christman, D. L.; Keim, G. I. *Macromolecules* **1968**, *1*, 358.

(22) (a) Doi, Y.; Ueki, S.; Keii, T. *Macromolecules* **1979**, *12*, 814. (b) Doi, Y.; Koyama, T.; Soga, K. *Makromol. Chem.* **1985**, *186*, 11.

(23) For example: Christman, D. L. *J. Polym. Sci., Part A-1: Polym. Chem.* **1972**, *10*, 471.

(24) CIF and XYZ files for V(NAd)Me₂[2-ArNCH₂(C₅H₄N)] (**2a**), V(NAd)Me(OR')[2-ArNCH₂(C₅H₄N)] [R' = OC(CF₃)₃ (**3a**), OC(CF₃)₂(CH₃) (**3b**), and OC(CH₃)₃ (**3c**)] are shown in the Supporting Information.

(25) Yamada, J.; Nomura, K. *Organometallics* **2005**, *24*, 3621.

(26) Zhang, W.; Nomura, K. *Organometallics* **2008**, *27*, 6400.

(27) Murphy, V. J.; Turner, H. *Organometallics* **1997**, *16*, 2495.

(28) Zhang, S.; Katao, S.; Sun, W. H.; Nomura, K. *Organometallics* **2009**, *28*, 5925.

(29) Reported examples for synthesis of cationic complexes by reaction of vanadium-methyl complex with [Ph₃C][B(C₆F₅)₄], [PhN(H)Me][B(C₆F₅)₄], B(C₆F₅)₃: Liu, G.; Beetstra, D. J.; Meetsma, A.; Hessen, B. *Organometallics* **2004**, *23*, 3914. Syntheses and structural analyses of the cationic complexes by reactions of V(N-2,6-Me₂C₆H₃)Me(NC^tBu)₂ with [Ph₃C][B(C₆F₅)₄], [PhN(H)Me][B(C₆F₅)₄], B(C₆F₅)₃ are also reported in ref 25.

(30) Examples for isolation of cationic Ti-methyl complexes for ethylene polymerization: (a) Jia, L.; Yang, X.; Stern, C. L.; Marks, T. J. *Organometallics* **1997**, *16*, 842. (b) Lee, H.; Jordan, R. F. *J. Am. Chem. Soc.* **2005**, *127*, 9384. (c) Lee, H.; Nienkemper, K.; Jordan, R. F. *Organometallics* **2008**, *27*, 5075. (d) Nienkemper, K.; Lee, H.; Jordan, R. F.; Ariafard, A.; Dang, L.; Lin, Z. *Organometallics* **2008**, *27*, 5867. (e) Itagaki, K.; Kakinuki, K.; Katao, S.; Khamnaen, T.; Fujiki, M.; Nomura, K.; Hasumi, S. *Organometallics* **2009**, *28*, 1942. (f) Hasumi, S.; Itagaki, K.; Zhang, S.; Nomura, K. *Macromolecules* **2011**, *44*, 773.

(31) NMR spectra in the reactions of V(NAd)Me₂[2-(2,6-Me₂C₆H₃)NCH₂(C₅H₄N)] (**2a**) with [Ph₃C][B(C₆F₅)₄] and V(NAd)Me(O^tBu)[2-(2,6-Me₂C₆H₃)NCH₂(C₅H₄N)] (**3c**) with B(C₆F₅)₃ are shown in the Supporting Information.

(32) Dixon, R. E.; Streitwieser, A. *J. Org. Chem.* **1992**, *57*, 6125.

(33) For examples:^{30a} (a) Nomura, K.; Fudo, A. *Inorg. Chim. Acta* **2003**, *345*, 37. (b) Keaton, R. J.; Jayaratne, K. C.; Fettinger, J. C.; Sita, L. R. *J. Am. Chem. Soc.* **2000**, *122*, 12909. In ref 30a, the resultant slurry solids in toluene, corresponding to cationic complexes, were filtered and isolated after dried *in vacuo*. (c) Synthesis of cationic zirconocene complexes containing alkoxy ligand by methyl abstraction with B(C₆F₅)₃: Wu, Z.; Jordan, R. F.; Petersen, J. L. *J. Am. Chem. Soc.* **1995**, *117*, 5867.

(34) Additional NMR spectra (in C₆D₆) are shown in the Supporting Information. Samples for NMR spectra were prepared by dissolving complex (ca. 20 mg) in toluene-*d*₈ or C₆D₆, followed by addition of prescribed Al cocatalyst in the dry box.

(35) Zhang, W.; Nomura, K. *Inorg. Chem.* **2008**, *47*, 6482.

(36) Solution XAFS (X-ray absorption fine structure) analysis [solution phase V K-edge XANES (X-ray absorption near edge structure) and EXAFS (extended X-ray absorption fine structure)] was conducted through the use of synchrotron radiation at SPring-8, BL01B1 beamline. More data including XANES, EXAFS spectra and curve fittings [by calculations on the basis of X-ray crystallographic structures of V(NAd)Cl₃, V(NAd)Cl₂[2-(2,6-Me₂C₆H₃)CH₂C₅H₄N] (**1**), V(NAd)Me₂[2-(2,6-Me₂C₆H₃)-CH₂C₅H₄N] (**2a**), and/or DFT calculations] were shown in the Supporting Information.

(37) (a) For example (account): Yamamoto, T. *Adv. X-ray Chem. Anal., Japan* **2007**, *38*, 45. The transition of a 1s electron to 3d orbital gives weak pre-edge peaks due to the electric quadrupole transition for any symmetries. An intense pre-edge peak is assigned to an electric dipole transition to p-character in the d-p hybridized orbital, and the mixing of a metal 4p orbital with the 3d orbital strongly depends on the coordination symmetry. Related references include: (b) Srivastava, U. C.; Nigam, H. L. *Coord. Chem. Rev.* **1973**, *9*, 275. and references cited therein.

(38) For example (solid structural analysis of vanadium compounds by XAS spectra): (a) Wong, J.; Lytle, F. W.; Messmer, R. P.; Maylotte, D. H. *Phys. Rev. B: Condens. Matter Mater. Phys.* **1984**, *30*, 5596. (b) Asakura, H.; Shishido, T.; Yamazoe, S.; Teramura, K.; Tanaka, T. *J. Phys. Chem. C* **2011**, *115*, 23653.

(39) A shoulder-edge peak observed at 5477.8 eV (**1**), 5476.4 eV (**1** + Me₂AlCl), 5474.7 eV (**1** + Et₂AlCl), and 5475.5 eV (**2a** + Me₂AlCl) might be considered as 1s–4p transition or ascribed to V–Cl bond. The latter explanation might be good agreement with decrease in the intensity upon addition of MAO (Figure 4a);³⁶ this would also be related to the fact that the intensity of V–Cl (coordination number) by FT-EXAFS spectrum decreased upon addition of MAO (Figure S3-8).

(40) As shown in Figure 3, the ⁵¹V NMR spectra of toluene-*d*₈ solution containing **2a** became broad upon addition of MAO (10 equiv) with decrease in the intensity of **2a**, and no clear resonances were observed upon further addition (50 equiv) due to two-phase separation (toluene-*d*₈ soluble/insoluble). In contrast, a toluene solution containing **2a** with MAO became homogeneous without phase separation. We have no clear explanation concerning the observed difference between the ⁵¹V NMR spectrum (in toluene-*d*₈) and the XANES spectrum (in toluene).

(41) A rather strong intensity of the pre-edge peak in V(NAd)Cl₃ is due to the tetrahedral geometry around vanadium (*e*_g < *t*_{2g}) dominant transition from 1s–3d transition to *t*_{2g}).³⁷ The shift of pre-edge and edge-shoulder peaks (1.3 eV) upon addition of Me₂AlCl would be due to formation of vanadium(IV) [and vanadium(III)] species, and the assumption would also supported by the ⁵¹V NMR spectrum and ESR spectrum.^{12b}

(42) As shown in Figure S3-8, EXAFS spectra for V(NAd)Cl₂[2-(2,6-Me₂C₆H₃)CH₂C₅H₄N] (**1**) and complex **1** in the presence of MAO, two peaks at 1.2 Å and 1.9 Å were observed. The backscattering amplitude for each peak in the complex **1**, obtained by reverse Fourier transform analysis, was compared with them of V–N and V–Cl bonds calculated by FEFF (Figure S3–10). The backscattering amplitudes for the peaks at 1.2 Å and 1.9 Å were close to those of the V–N and V–Cl bonds, respectively. Therefore, we determined that the peaks at 1.2 Å and 1.9 Å are the V–N and V–Cl bonds, respectively. The peak intensity of the V–N hardly changed by the addition of MAO whereas that of the V–Cl bonds was reduced in Figure S3–8. Same results were obtained for curve fitting analysis as shown in Tables S3–1 and S3–2. This change indicates that the coordinated Cl of the complex **1** was removed by the reaction with MAO without any changes for V–N bonds. Detailed data were shown in the Supporting Information. We appreciate the reviewer for suggestion placing more analysis data in the manuscript.

(43) SIR2008 Burla, M. C.; Caliendo, R.; Camalli, M.; Carrozzini, B.; Cascarano, G. L.; De Caro, L.; Giacovazzo, C.; Polidori, G.; Siliqi, D.; Spagna, R. *J. Appl. Crystallogr.* **2007**, *40*, 609.

(44) Crystal Structure 4.0: Crystal Structure Analysis Package; Rigaku and Rigaku Americas: Tokyo, Japan, 2000–2010; pp 196–8666.

(45) SHELX97: Sheldrick, G. M. *Acta Crystallogr., Sect. A: Found. Crystallogr.* **2008**, *64*, 112.10.1107/S0108767307043930